IEEE Access
Multidisciplinary ⋮ Rapid Review ⋮ Open Access Journal

Received November 26, 2015, accepted December 18, 2015, date of publication January 20, 2016,
date of current version March 4, 2016.

Digital Object Identifier 10.1109/ACCESS.2016.2518190

INVITED PAPER

Toward Label-Free Biosensing With Silicon Carbide: A Review

OREN COOPER[1], BEI WANG[2,3], CHRISTOPHER L. BROWN[2], JOE TIRALONGO[1], AND FRANCESCA IACOPI[2,3], (Member, IEEE)

[1]Glycomics Institute, Griffith University, Southport, QLD 4222, Australia
[2]Queensland Micro and Nanotechnology Centre, Griffith University, Nathan, QLD 4111, Australia
[3]Environmental Futures Research Institute, Griffith University, Nathan, QLD 4111, Australia

Corresponding author: F. Iacopi (f.iacopi@griffith.edu.au)

This work was supported in part by the Air Force Office of Scientific Research, Office of Naval Research Global, and Army Research, Development and Engineering Command through the AFOSR/Asian Office of Aerospace Research and Development under Grant 15IOA053 and in part by the Australian National Fabrication Facility, Queensland Node. The work of F. Iacopi was supported by the Australian Research Council under Grant FT120100445.

ABSTRACT Recent innovation in microelectrical–mechanical systems (MEMSs) and plasmonics-based technologies has opened up perspectives for label-free sensing of biological and chemical analytes. Label-free sensing would enable increased sensitivity and miniaturization capabilities for biosensing devices. Silicon carbide is a semiconductor material that happens to possess ideal properties for augmenting both the MEMS/nanoelectromechanical systems and the plasmonics routes. It has remarkable chemical and biological inertness resulting in a high degree of biocompatibility, as well as pronounced mechanical resilience. In addition, it is an efficient (low loss) plasmonic metamaterial. Its cubic polytype can be grown on silicon wafers, allowing easy micromachining into building blocks for sensing devices, scalable to large volume production. Finally, silicon carbide is an ideal starting material for a controlled, wafer-scale growth of graphene, offering an additional wealth of excellent properties for nanosensing. The combination of all of these capabilities makes silicon carbide an outstanding material platform for the realization of label-free, analyte-specific, and highly sensitive biochemical molecule detection systems. These technologies will open exciting horizons in terms of high throughput, efficient drug screening, and early pathogen detection.

INDEX TERMS Silicon carbide, biosensing, label-free detection, graphene, micro-electro-mechanical systems, cantilevers, biocompatibility.

I. INTRODUCTION

The development of label free, highly sensitive and molecule specific analyte detection technologies is of high relevance for a number of applications in the bio-medical area, including medical diagnostics and drug screening. Therefore, the availability of a robust, bio-compatible functional material which can be structured into a miniaturized sensing device is highly desirable. Such a system would enable highly efficient, high throughput chemical analysis and potentially minimally invasive endoscopic sensing. Silicon carbide is a wide band-gap semiconductor [1]–[3], with demonstrated bio- and hemo- compatibility [4]–[8]. Also, similar to silicon, the silicon carbide surface can be functionalized to capture or bind with specific reagents, and its use has been demonstrated in neural probes, enabling among others applications such as brain-machine interfaces [9]. Moreover, silicon carbide is a suitable template for the direct growth of epitaxial graphene, likely also a bio-compatible material which can bring exciting additional functionalities and capabilities to the silicon carbide system, such as low-loss plasmonic technologies [10].

This paper will first present a review of the status and recent progress in the area of label free detection technologies. We will focus on optical (plasmonics) and microelectrical-mechanical (MEMS) based sensing, as potentially the most accurate and molecule-specific sensing technologies, indicating advantages and limitations. A general introduction on silicon carbide will follow, focusing on how this wide band-gap semiconductor, as well as its combination with graphene, can further this field and open exciting horizons for bio-medical applications.

II. LABEL FREE DETECTION

Current established DNA [11], protein [12], [13], glycan [14], [15] and lectin [16], [17] arrays allow for

2169-3536 © 2016 IEEE. Translations and content mining are permitted for academic research only.
Personal use is also permitted, but republication/redistribution requires IEEE permission.
See http://www.ieee.org/publications_standards/publications/rights/index.html for more information.

high-throughput multiplexing with reduced sample volume. However, without appropriate quantitative controls and complex algorithms [18], results remain qualitative due to the requirement for fluorescent, photochemical or radioisotope tagging [19]. These labels and their appropriate laser scanners are commercially available, however, background interference due to the label itself and the need for adequate signal controls are serious limitations to this technology. Labelling probe molecules for large-scale studies is tedious, expensive and limited by various factors. For instance size and position of the label can induce conformational strains and steric hindrance, affecting the probes ability to interact with target structures [20]. These factors become exacerbated when probe molecules (metabolites, oligonucleotides, peptides and small organic molecules) are smaller than the label being used. Non-specific binding to the array platform will also contribute to the intrinsic fluorescence being measured and can give rise to false positives. Finally the extent of fluorescent labelling also needs to be optimized for various probe molecules to ensure normalisation between results. Using the established array technology in combination with real time label free detection systems would enable a paradigm shift within molecular and structural biology.

Accordingly, advances in label free detection methods are highly desirable for next generation bio-sensing platforms due to their potentials for increased sensitivity and direct measurement [21].

A. PLASMONIC SENSORS

From the discovery of surface plasmons in 1968 [22], plasmonic materials have emerged offering next generation label free detection. Plasmonic materials possesses a negative real and small positive imaginary dielectic constant, capable of supporting a single guided mode of electromagnetic field [21], [23]. Here the energy and momentum of a photon is coupled to a free electron gas in the form of surface plasmons. The surface plasmon is transversely magnetic; as such the vector of the magnetic field lies in plane of the metal-dielectic interface and is perpendicular to the direction of propagation. This is possibly due to surface plasmon sensitivity to the refractive index changes around metallic structures by electromagnetic radiation at a metal-dielectric interface [23], [24].

Plasmon based resonance sensing can be broadly separated into two types; the first is propagating surface plasmon resonances (PSPRs) that rely on evanescent electromagnetic waves bound by planar metal-dielectric interfaces. The second type is localized surface plasmon resonances (LSPRs), where electromagnetic waves are confined on metallic nanostructures [25]. Unlike conventional optical sensors that rely on labels (fluorophore and chromophore), surface plasmon resonance can transduce the binding event due to changes in the local refractive index when the target analyte binds to the surface.

Since the realization in 1980 that surface plasmon resonance (SPR) could be an outstanding probe of surface chemistry [26], this technique has been extensively used to elucidate binding kinetics, conformational changes and quantifications of chemicals; small ions and biomolecules immobilized to the surface [27], [28]. Use of thin metallic film allows plasmons to propagate hundreds of micrometers along the metal surface with an associated electric field that decays exponentially allowing for detection of refractive index through intensity, wavelength or angle shifts. Enhancements in this field have seen detection below the submicrometer range from improved molecular adsorptions [29]–[31], enlargement of binding site [32], [33] and introduction of signal enhancers on the metal surface [34]–[36]. SPR is a versatile tool as the monitored optical parameter can vary based on user specification including; measurement of the wavelength where resonant coupling occurs; the phase of the light; and the intensity of binding based on measurement of the shift in the angle at which resonant coupling takes place [37], [38]. Conventional SPR has long been the technology of choice for label free detection [39], however it does not match the demands of current microarray technology; being unable to couple the high throughput platform with sensitivity [40]. Conventional SPR is also significantly expensive as multiplexing relies on only a few flow cells limiting analysis to 50 spots [41]. Alternatively LSPR offers a cheaper alternative for smaller laboratories due to integration of lab-on-chip (LOC) technologies [42]. LOC technologies allow for cheaper purchase of one-time assays capable of producing vast quantitative bioinformation.

LSPR confines excited electromagnetic waves onto metallic nanostructures and by controlling physicochemical properties the spectral position and magnitude can be altered. Optimization of size, shape, composition, interstructural spacing and local dielectric environment have led to the advent of gold nanorings [43]–[45], metallic nanoislands [46], [47] and nanoholes in thin gold films [31], [48]. Unlike PSPRs, these nanostructures show enhanced sensitivity, as there is less interference from the bulk refractive index [32], [49], [50]. In addition to the refractive sensitive capability of LSPR, electromagnetic field enhancements generated around them has been shown to be ideal when coupled with surfaced enhanced Raman scattering (SERS). Nanosphere lithography (NSL) used to develop nanoparticle arrays (most commonly triangular structures) with tuneable LSPR has been previously developed as a self-assembled monolayer [34], [36]. Both experimental and theoretical studies have demonstrated that the sharp tip nanotriangles create an electromagnetic enhancement factor as large as 10^8 [37], [38]. Further advances have seen atomic layer deposition with alumina overlayer to particles fabricated via nanosphere lithography, resulting in significant increases in thermal stability [43], [51]. The electromagnetic mechanism of SERS does not require direct contact of the surface due to the electric field extending within a few nanometers of the surface. Enhancement of Raman scattering can be exploited to measure systems that require surface-immobilized biological molecules [46], [52] however research is still

required to enhance the multiplexing capabilities of this platform.

However, the current metal-based plasmonics sensing technologies are strongly limited by high resistive losses, which have restricted the development of these devices. Approaches to minimize metallic losses through discovery of better plasmonic materials offer promising alternatives, via doping, alloying and careful band structure engineering [53], [54]. As such low-loss plasmonic metamaterials have emerged with longer plasmon lifetimes [55]–[58]. This category of low–loss materials include silicon carbide and graphene as both are tunable and have carrier concentrations high enough to provide a negative real permittivity [55].

B. MEMS CANTILEVER SENSORS

Micro-electro-mechanical systems (MEMS) offer an alternative approach for quantitative molecular recognition. These systems rely on silicon and wide-bandgap (WBG) semiconductors that allow for increased stability, biocompatibility and further miniaturization for resonant nanoelectromechanical systems (NEMS) [59], [60]. The ability to detect multiple target molecules in small sample volumes has maintained a significant relevance for research into early detection of disease, and therefore platforms that satisfy these requisites are appealing. Microcantilevers arrays have emerged as a very promising candidate for label free multi-target detection that is both sensitive and selective in small volumes of sample. MEMS cantilever sensors are another next generation platform readily fabricated on silicon wafers [48], [61]. An array can be fabricated through a ''top-down'' approach to release spring microbeams. These cantilevers typically measure approximately 50-200 μm long, 10-40 μm wide and 0.3-3 μm thick and respond to surface stress variation from chemical or biological process [50], [62]. Cantilevers can be designed with very small force constants (0.008 - 30 N/m) making them extremely sensitive to variations in adsorption of molecules [63], [64].

Capture of a molecule onto the surface of a cantilever can be measured thanks to the deflection of the cantilever from adsorption-induced forces. In a dynamic regime, mass adsorption on the surface of a microbeam can result in an observable shift from its natural resonance frequency, as a mass change will affect the spring constant of the system [65]. Both adsorption induced cantilever deflections and frequency shifts can be monitored simultaneously [51]. Initially cantilevers were not considered very promising mass sensors due to non-uniformities in non-specific binding over the entire length of the cantilever resulting in variations in spring constant. However, by designing cantilevers with a localized adsorption area at the terminal end of the cantilever the contribution of the differential surface stress can be entirely attributed to mass loading [66]. The resonance frequency can shift due to changes in mass and spring constant. Surface area has been shown to increase sensitivity of mass detection, leading to nanopatterning and nanofabricated holes for increasing the total absorbed mass [61]. Despite being well suited for mass detection in air and vacuum, detection of absorbed mass under solution is best detected through surface stress variations; due to poor resolution of cantilever resonance frequency in liquid environments [62]. In general deflection of cantilever can be divided into two different modes for detection; static and dynamic.

1) CANTILEVER DEFLECTION-BASED SENSING

a: STATIC DETECTION

Static mode of deflection is a result of variations in surface stress on the opposing surface of the microcantilever. Surface stress variations exist as changes in surface energy density or tension, occurring through molecule adsorption that decreases surface free energy. By restricting adsorption to one side of a cantilever, a differential surface stress between each side of the beam is produced, leading to cantilever bending. This surface stress can be explained by Stoney's formula [67], which shows that the longer the cantilever the more sensitive it becomes to surface stresses *(see figure 1)*. The sensitivity also relies on the detection technique. Optical detection techniques are most commonly used; however they are limited due to a narrow dynamic range and parasitic deflection [68]. As such the dynamic mode of detection is more beneficial being insensitive to the drift of the deflection signal and increasing reproducibility.

b: DYNAMIC DETECTION

The dynamic mode of detection is directed at the variation in vibration frequency of the beam due to specific adsorption [69]. Unlike static measurements of surface stress, cantilever deflections leads to a ''dynamic'' action that can be used to quantitatively detect mass loading. Microcantilever beams freely resonant at their natural frequency due to thermal excitation. Mass loading leads to a decrease in vibrational frequency allowing for direct measurement by plotting the displacement amplitude against frequency [70] (*see figure 1 b*). Each resonance mode has its own quality (Q) factor that indicates the sharpness of a resonant peak [71]. Q factors are liable to damping effects from both liquid environments and geometry of the cantilever which can lead to poor frequency resolution [72], [73]. Higher Q factors allow for lower minimum detectable resonance shifts.

c: READ OUT MECHANISMS

In the last decade many techniques to measure cantilever resonance or deflection, have been demonstrated including; optical beam deflection [63], [74], [75] piezoresistivity [21], [76]–[78]; piezoelectricity [27], [28]; electron tunneling [79], [80] and capacitance [81]. Optical beam deflection was the first reported technique to exploit the mechanics of cantilever deflection by measuring bending by reflecting a focused beam of light from the tip of the cantilever into a position-sensitive detector. Optical beam deflection is a popular method for detection due to its sensitivity to capture cantilever bending in the sub-nanometer

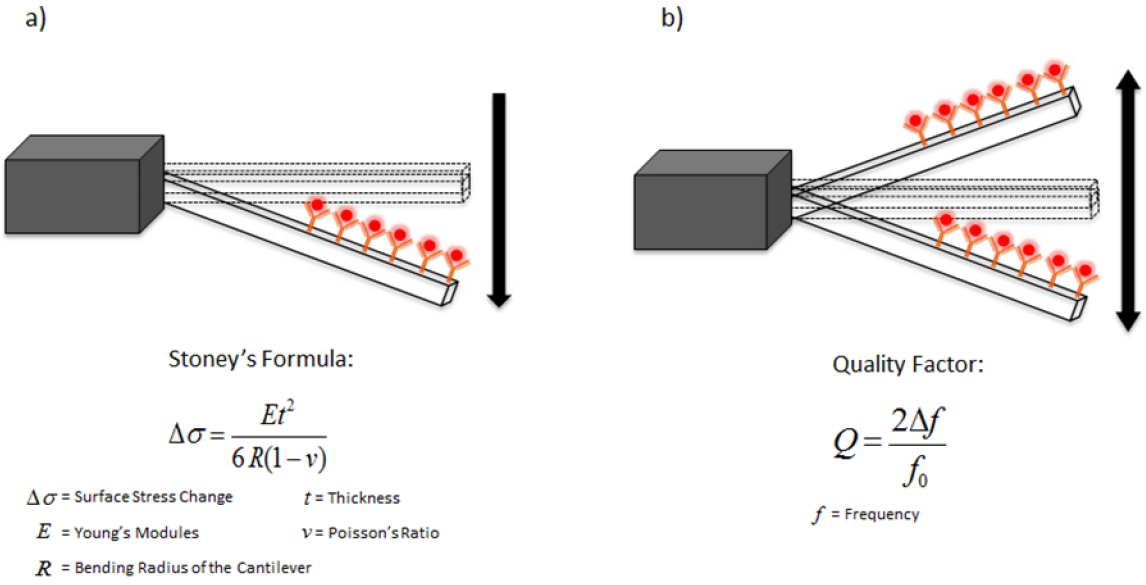

FIGURE 1. Schematic of the two different cantilever deflection based sensing. (a) Static detection through changes in surface stress. (b) Dynamic detection through changes resonance frequency.

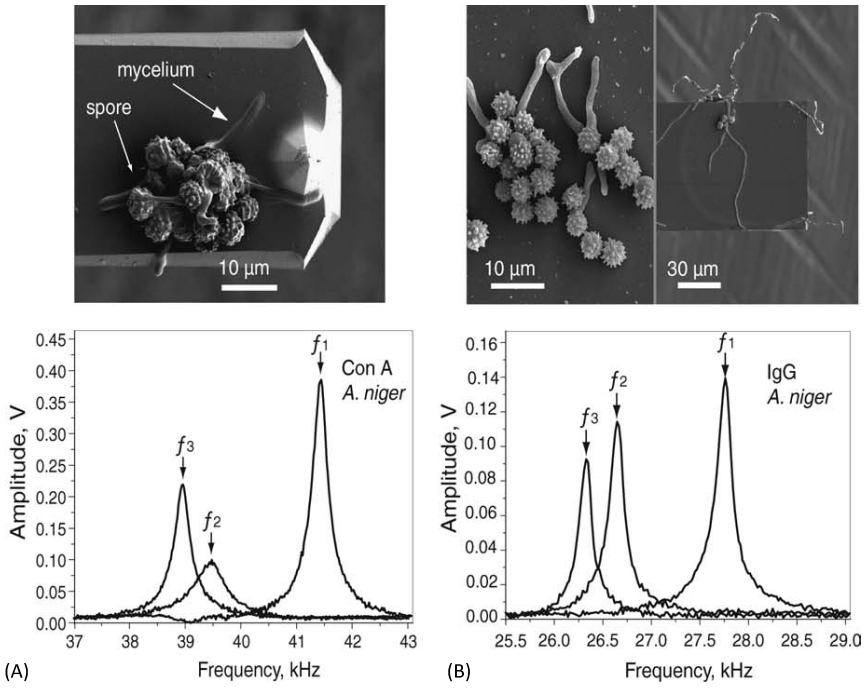

FIGURE 2. Scanning electron microscopy images of immobilized fungal spores and corresponding frequency spectra of the cantilevers after spore immobilization and spore growth. (A) Mycelial fungus *Aspergillus niger* on Con A coating; mycelia growing from spores after 12 hours (B) *A. niger* on IgG coating, active mycelial growth from spores (left image—growth time 4 h, right image—growth time 9 h). Resonance frequencies: f_1—unloaded cantilever, f_2 —cantilever with immobilized spores, f_3 —cantilever with growing immobilized spores after exposure. The first resonance frequency shift $\Delta f_1 = f_1 - f_2$ corresponds to fungal spore mass loaded on the cantilever; second shift $\Delta f_2 = f_2 - f_3$ corresponds to *A. niger* mycelial growth. Reprinted with permission from [107].

range [82]–[84]. A beam from a solid-state laser diode is focused onto the apex of the cantilever leading to a reflection that is captured by a positive sensitive detector of two closely spaced photodiodes. A differential amplifier captures this output signal and the measured distance traveled by the reflected laser beam is calculated proportionally to

cantilever bending. Unfortunately this method relies on a complex design system, which can prove expensive to manufacture.

Piezoresistivity is an effect that semiconductors such as silicon and silicon carbide show as an intrinsic resistance change sensitively as a function of bending. A piezoresistive detection approach, measures the resistance of the material, which varies as a function of applied stress. The length of a piezoresistive cantilever again dictates resistance with a range typically between 1-5 kΩ. Ramussen *et al.,* (2003) developed multilayer cantilever beams with single crystal silicon as the active functional element to detect variations in resistance as a function of deflection. Silicon doping of the beams was restricted to the neutral axis and the active silicon sandwiched between an insulating layer of silicon nitride and silicon dioxide. Cantilevers fabricated to this design with an insulating layer enable highly sensitive piezoresistive detection in liquid environments [85]. Increases in sensitivity have also been achieved by reducing the thickness of a cantilever. Piezoelectrical detection is possible by coating cantilevers with piezoelectric materials to generate a measurable charge in response to cantilever bending [86], [87]. A drawback to this technique is the extensive fabrication due to encapsulation of the electrically active parts.

Lee *et al.,* (1995) devised a self-excited piezoelectric cantilever by sandwiching a thin piezoelectric film of zinc oxide between two aluminum layers. Gravimetric testing revealed high sensitivity for the detection of chemical vapor concentration and relative humidity using an acoustic output transducer [88]. Using millimeter sized cantilever sensors, Campbell & Mutharasan (2006) demonstrated detection of *Bacillus anthracis* spores in liquid medium under both stagnant and flow conditions. These cantilevers were very sensitive with detection down to 300 spores/mL, as well as highly selective for *B. anthracis* in a mixture with *Bacillus thuringiensis* spores at ratios up to 1:500 [86]. Another work by Hwang *et al*., (2004) fabricated self-sensing piezoelectric cantilevers for detection of prostate specific antigen (PSA). Using a PSA antibody immobilized to a calixcrown self-assembled monolayer, they were able to show the resonance frequency shift of the cantilever was proportional PSA concentration [68]. This group also employed the same fabrication technique using an immobilized C reactive protein antibody to detect C-reactive protein [89].

C. BOTTOM-UP CHEMICAL NANOSENSORS WITH NANOTUBES AND NANOWIRES

Nanotubes and nanowires are one-dimensional nanostructures that have attracted increased interest as NEMS elements fabricated using a ''bottom-up'' approach. These structures contain excellent intrinsic properties and a low dimensionality. Wagner & Ellis (1965) first discovered nanowires (NW) through vapor-liquid-solid (VLS) mechanism by depositing semiconductor atoms under a supersaturated liquid catalyst to grow an epitaxial wire [90]. Since this innovation, the growth of many different NWs using VLS has been fabricated using various semiconductor atoms such as; Si, SiC, GaAs, Ge, and GaN [91]–[94]. A study by Cui Y *et al.,* (2001) developed boron-doped silicon nanowires (SiNWs) to create a highly sensitive, real-time electrically based sensor [95]. In 2004 Patolsky *et al.,* using this same principal was able to show binding of a single virus particle [96]. The nanowire sensing approach is advantageous over conventional SPR in terms of sensor packing densities, demonstrating the ability to incorporate 2400 nanowire sensors onto one array [97]. This allows for reduced sample volume coupled with a higher sensitivity and high throughput function. Gamby *et al.,* (2009) fabricated gold NW (170 nm in diameter) in a polycarbonate microchannel through electrocrystallization techniques. These NWs demonstrated a measurable increase in Raman cross-section and could serve as a SERS active dielectric sensor easily integrated into lab-on-chip systems [52]. Nanowires are also suitable biological materials as they don't display acute (100 hr) toxicity towards cells, in fact, cells are capable of degrading NW into aggregates within days [98].

Carbon nanotubes (CNTs) are hollow variants of solid NW structures; first discovered by Iijma (1991), CNTs initially generated interest in the field of nanoelectronics due to their superconductivity capabilities [99]. Since their advent nanotubes have undergone extensive theoretical and experimental application to tailor desired growth and electronic properties [100]–[102]. Similar to MEMS structures nanotubes have comparable thermal and electrical conductivity and can be grown through CVD. CNT electrical properties can be controlled through chirality and number of carbon layers [42], [103]. Studies have demonstrated CNTs are useful label free immune sensors; for instance Okuno *et al.,* (2006) fabricated a single walled carbon nanotube (SWNTs) array to detect total PSA using differential pulse voltammetry. These single walled carbon nanotubes increased electron transfer improving the limit of detection to 0.25 ng/mL [100]. Silicon carbide nanotubes (SiCNTs) were first synthesized 10 years later by Pham-Huu *et al.,* (2001) and often advantageous over CNTs, particularly with respect to stability at high temperature, ease for sidewall decorations and semiconducting potentials irrespective of chirality [103]. SiCNTs have been shown to be exceptional in the detection of harmful gases, including; CO, NO [104], [105] and HCN [103]. Using SiC for fabrication of SiCNTs introduces interesting magnetic and electrical properties which can be manipulated by varying the surface decoration with SiH_3 and CH_3 functionalities [102].

D. BIOLOGICAL APPLICATIONS

Microcantilever LOC platforms capable of detecting antigen-antibody interaction [50], protein-protein binding [106], DNA hybridization [64], [74] and DNA-protein interaction [83] have already been fabricated. Microcantilevers offer a comparable bimolecular detection platform to perform such multiplexing and label free analysis of these biomolecules with unparalleled sensitivities. As cantilever bending is sensitive enough to register the free energy change induced

from binding events; as such immobilization of antibody molecules, leads to measurable cantilever deflection. For example ssDNA can be immobilized on the gold side of an asymmetrically doped cantilever using a thiol linker. This adsorption of ssDNA results in a surface stress variation between 30-50 mN/m [64], [74]. This ssDNA can be used as a probe to detect complementary sequences and would serve as an adequate platform to detect mutations such as single nucleotide polymorphisms [83], [107].

Fritz *et al.,* (2000) demonstrated optical beam deflection technique to detect nucleic acid hybridization on gold-coated silicon cantilevers. A 5-thio modified synthetic DNA oligonucleotides with different base sequences were immobilized and later detected in liquid through surface stress shifts of asymmetrical doping leading to cantilever deflection. In this same work it was shown that these cantilevers were able to distinguish between complementary oligonucleotides and a pair with single base mismatch between the DNA sequences being detected [74]. Advances on this principle led to the monitoring of restriction and ligation of cantilever coated with DNA. Stevenson *et al.,* (2002) functionalized silicon cantilevers coated in gold with 3-aminopropyltriethoxysilane (APTES) to monitor restriction and ligation of DNA. An oligonucleotide with the *Hind*III restriction site was immobilized to the APTES monolayer, followed by digestion with *Hind*III. This scission led to cantilever negative deflection due to the shortened oligo with a single stranded sticky end. Subsequent hybridization with a suitable second oligo in the presence of ligase and thus extension of immobilized DNA led to a commensurate cantilever deflection in the opposite (or positive) direction due to increases in mass loading [107].

Ilic *et al.,* (2000) was the first to report a high sensitivity detection of *Escherichia coli* using antibody layer coated silicon nitride cantilevers. The resonant frequency shifts measured as a function of mass loading from cell depositions was correlated with the number of cells bound on the surface [108]. Building on this work, Ilic *et al*., (2004) were also the first to demonstrate detection of Baculovirus particles bound selectively to an AcV1 antibody monolayer immobilized onto cantilevers. These piezoelectric cantilevers allowed for single virus particle detection by measuring the resonant frequency shift [109]. Gfeller *et al*., (2005) realized the cantilever biosensing potential for rapid real time detection of label free *E. coli* growth by coating cantilevers in nutritive agarose with bacteria. Resonance frequency shifts due to increasing mass were matched to the conventional bacteria growth curves, sensitive enough to observe all characteristic phases. A high sensitivity of 50 pg/Hz was calculated to be approximately 100 *E. coli* cells. These cantilevers were also shown to augment the ability to rapidly assess antibiotic resistance by either incorporating or omitting antibiotic coating on the cantilever [110].

Nugaeva *et al.,* (2004) using silicon cantilevers coated with 30 nm of gold functionalized with concanvalin A, fibronectin or immunoglobulin G demonstrated spore immobilization and germination of mycelial fungus *Aspergillus niger (see figure 2)*. Shifts in resonance frequency could be detected within a few hours as opposed to several days. Biosensing capabilities of these cantilevers detected fungi in the range of 10^3 – 10^6 CFU/mL, and thus would be suitable for use in medical and agricultural diagnostic for both food and water quality monitoring [111]. Savran *et al.,* (2004) immobilized anti-Taq aptamer to silicon nitride cantilevers to investigate Taq polymerase binding affinity. Various concentrations of Taq polymerase (0.3-500 pm) was applied to the cantilevers resulting in polymerase aptamer binding and subsequent induce surface stress and deflection (3-32 nm depending on concentration) [112]. The resulting curve was fit using the least-squares method to reveal a K_d of ∼15 pM which was comparable to previous reports performed in solution [113]. Glucose detection has also been performed with glucose oxidase coated cantilevers [114]–[116]. These examples emphasize the high sensitivity and high throughput capabilities of microcantilever array platforms. The principles of surface plasmon resonance applied to these microstructures realize the potential of real time miniaturized multiplexing assays.

III. SILICON CARBIDE

A. BASIC PROPERTIES & POLYTYPES

Moissianite, an extremely rare crystal formation of silicon carbide (SiC), is typically found in minute quantities in corundum deposits, kimberlitic and meteorites. SiC is a tetrahedron of four carbon atoms covalently bound to a centre silicon atom resulting in a 2-dimensional polymorphism. The high mechanical and chemical stability of SiC can be attributed to very short bond lengths, as each carbon is located 3.08 Å from each other and 1.89 Å from the silicon which leads to a very high bond strength [49], [117]–[119]. Si and C can form a bilayer introducing a double layer-stacking variable that defines over 200 different polytypes of SiC. These polytypes have been characterized based on the SiC bilayers that can assume a different hexagonal frame lattice and stacking sequence (*see figure 3*). 4H- and 6H- SiC are hexagonal polytypes based on the 4 and 6 respective bilayers required for the basic structure; alternatively, 3C-SiC (β-SiC) is an example of a cubic polymorphic structure comprised of 3 bilayers [120], [121].

SiC is a family of wide band gap (WBG) semiconductors, where organization of bilayers confers band gap energy exclusive to each polytype; 2.39 eV for 3C-, 3.265 eV for 4H- and 3.023 eV for 6H-SiC [1], [49]. These different properties have led to diverse applications across polytypes; 4H-SiC with the highest band gap is suited for power electronic devices, whilst 6H-SiC, due to a similar lattice constant to that of gallium nitride, is best suited in advancements in LEDs [122] Alternatively, 3C-SiC heteroepitaxially deposited on silicon wafers has successfully been used in the generation of MEMS cantilevers [123]; with promising perspectives of further downscaling towards NEMS [60], [124]. SiC's explored bio- and hemo- compatibility make it an

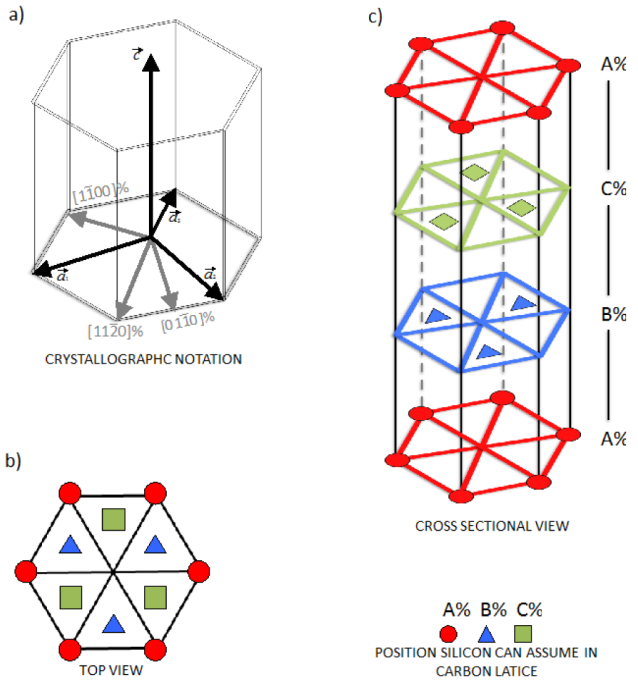

FIGURE 3. (a) Hexagonal crystallographic notation, which is used for SiC crystals independent of the actual lattice symmetry. It is based on four Miller-Bravais indices a_1, a_2, a_3 and c (shown in black) where: $a_1 + a_2 + a_3 = 0$. The grey vectors denote the different crystal orientations. (b) Illustration of the three different positions that the hexagonal frame of SiC bilayers can assume in the lattice. (c) ABCABC... stacking sequence of cubic 3C-SiC (zinc blende structure).

excellent candidate material for the for advancements in brain machine interfaces [4], [5]. The authors suggest [125] as an excellent review on advanced biomedical applications using SiC.

B. SYNTHESIS OF SiC

Recently, increased attention to SiC as a suitable material in numerous biomedical applications due to its WBG, chemical inertness and mechanical strength [126] has been realized as potential biotransducers in biosensors [4], [87], [125]. The main hexagonal polytypes of SiC can be grown as single-crystal ingots, from which SiC wafers can be obtained. Various methods are available to grow homoepitaxial single crystalline SiC films commonly through chemical vapour deposition (CVD) [118], [127]–[130] and less commonly through liquid phase epitaxy (LPE) [131] and molecular beam epitaxy (MBE) [132]. The 3C-SiC polytype is the only one that can be grown hetero-epitaxially on silicon. This is particularly advantageous as fabrication on silicon is well established and widely available. Growth on silicon can typically be achieved through three steps: firstly removal of native oxides present through hydrogen surface etching, a carbonization step to bond C to the Si dangling bond to create the first SiC "buffer" layer, and finally using a Si:C ratio of 0.7 to grow a cubic single-crystal layer on the buffer layer [118]. Modification to these steps such as the inclusion of silane between carbonization and growth steps has led to the production of very high quality films [133]. Advancements in surface preparation have led to the development in numerous techniques including; oxidation [117], [134]; sublimation etching [120], [135]; photoelectrochemical etching [136]; chemomechanical polishing [137], [138]; plasma etching [139] and hydrogen etching [128], [140], [141].

Growth of heteroepitaxial 3C-SiC films on silicon with high quality is still to-date very challenging because of the large lattice and thermal mismatch between the films and the silicon substrate [3]. Poly-SiC on the other hand has been shown to be more versatile capable of growth on diverse substrates at lower temperatures (500-1200 °C) and has allowed for the generation of multiple growth protocols. Production of SiC nanoparticles is again different; an electrochemical method by Wu *et al.*, (2005) involved etching of polycrystalline 3C-SiC coupled to ultra -sonication to yield an average particle size of 3.9 nm [142]. Similar electrochemical anodization etching coupled to mechanical grinding of nanoporous 6H-SiC also yielded 6H-SiC nanocrystals [143]. Lin *et al.,* (2008) used a low temperature, low pressure plasma reactor to synthesize amorphous SiC; subsequent annealing of the samples in argon at 800 °C yielded β-SiC nanoparticles ($<$10 nm) and graphite [144]. The amorphous phase of SiC allows for adjustable Si and C stoichiometry. Alternatively, Leconte *et al.,* (2008) used inductively coupled plasma to control synthesis of β-SiC nanopowders. Here, the SiC stoichiometry was controllable by the process pressure and the addition of methane to compensate the decarburization process [145]. Yang *et al.,* (2011) used laser ablation of Si in ethanol to produce 3C-SiC nanoparticles in a water suspension [146]. A study by Botsoa *et al.,* (2008) demonstrated the application of 3C-SiC quantum dots for living cell imaging. They synthesized 3C-SiC nanoparticles less than 10 nm in size through electrochemical anodization of polycrystalline wafers followed by successive grinding and finally centrifugation and were verified to have a non-toxic effect to the cell [147].

C. IMMOBILIZATION OF BIOMOLECULES

Current molecular recognition systems require the immobilization of biomolecules through covalent attachment [134], [148], [149] with specific attention to structural order and composition to maintain biological activity to maintain sensitivity towards chemical stimuli [150], [151]. This happens through surface functionalization for controlling the surface chemistry of the substrate itself and is therefore specific to the selected semiconductor material. For example the surface functionalization of silicon dioxide (SiO_2) has been shown to be unsuitable in electrolytic solutions [152] as well as conferring high noise levels in field effect transmitters (FETs) [153]. A study by Spetz *et al.,* (2006) exploited the thermal resistance properties of SiC to fabricate FET gas base sensors that operate at ∼1,000 °C [2]. A more recent paper by the same group built on this principle engineering a multifunctional sensor device with an integrated transistor and resonator, to measure NO metabolism in an individual's breath [154].

SiC has emerged as a promising biosensing material due also to the possibility of realizing a thin surface oxide, which is essential for the surface termination required to immobilize biomolecules. Passivation of the SiC surface can be realized through high quality monolayers with reactive sites generated either with a terminal hydrogen (H) or hydroxide (OH) surface [119], [128], [155], [156]. Theoretical studies by Preuss *et al.*, (2006) compared pyrrole-functionalized Si- and C-terminated SiC surfaces. They concluded that adsorption occurred through N-H dissociation and formation of N-Si bonding on the Si face however this was unstable on the C face most likely due to negative adsorption energy [157]. Similar *ab inito* computational chemical investigations chemical investigations by Cicero and Catellani also demonstrated a larger stability on the Si face of the SiC(001) surface compared to those on Si [158], [159]. A study by Schoell *et al.*, (2008) used self-assembled monolayers (SAMs) for functionalization of n-type 6H-SiC to the Si face. Covalent functionalization on patterned aminopropyldiethoxy-methylsilane (APDEMS) monolayers was later verified through immobilized fluorescently labelled proteins [155]. Williams *et al.*, (2012) also immobilized streptavidin via biotinylation on to APTES functionalized 4H-SiC (0001). To ensure immobilization; X-ray photoelectron spectroscopy (XPS), ellipsometry, contact angle and fluorescence microscopy was used to optimize APTES layer on the SiC surface. Notably, instead of performing a pirhana dip, hydroxylation occurred through oxygen plasma treatment with O_2:Ar (20:80) to grow a thin oxide layer [148]. Similar functionalization has been performed on 4H-SiC (0001) with mercaptopropyltrimethoxy-silane (MPTMS) and verified using XPS and water contact angle measurements [150]. Electrical contribution from APTES and MPTMS organic layers on 4H-SiC has been further evaluated and shown to exhibit a Schottky diode like I-V characteristic [134].

Numerous studies have been performed on the biosensing capabilities of the semi-insulating hexagonal polytypes (4H- & 6H-SiC) due to their low leakage, transparency and biochemical inertness [160]; however 3C-SiC has emerged as the polytype of choice. It is ideal for biomedical MEMs devices as it is less expensive and less polar when compared to 4H-, 6H-SiC [125], [161]. 3C-SiC has a well-defined surface for electron transfer due to a low gradient and in-plane stress from the closely packed cubic structure [162]. Coupled to high Young's modulus, 3C-SiC can be constructed into wide frequency resonators as cantilevers or bridge structures as detections methods for mass, gas and biomolecule identification.

D. SiC FOR BIOSENSING: DESIGN CONSIDERATIONS

Extensive research has shown that SiC is a superior alternative to Si, due to its demonstrated biocompatibility [2], [4], [125], [134], [154], [163]. Moreover, as it can be deposited on silicon wafers, its micromachining into MEMS building blocks is straightforward. SiC Young's modulus are notably high (440 GPa), as well as breakdown field twice as large as Si ($\sim$2 $MVcm^{-1}$) [136]; making SiC ideal to augment and even replace Si. In addition to this due to SiC chemical inertness [121], it is a suitable material in high temperatures, hostile environments and shows a high resistance to corrosion in body fluids [119], [128], [135], [155], [156], [164]–[166]. SiC's high elastic modulus (424 GPa), high hardness (5.8 GPa) and low friction coefficient (0.17) make it ideal as an *in vivo* biosensor and smart implant [163], [167]. Li *et al.*, (2005) used a nanoscale approach to characterize both the mechanical and tribological properties of SiC for orthopaedic applications [135]. Coupled to the electrical, mechanical and thermal properties of SiC reinforces its suitability as a biosensing substrate. These qualities alone, including the aforementioned WBG, increases the sensing capabilities of SiC as a semiconductor. Of the polytypes, 3C-SiC has demonstrated a major advantage in biosensing applications due to the reproducibility of quantitative surface modification and functionalization. This has been realized as a versatile format for immobilization of biomolecules with high reproducibility in bioanalytical applications.

Fabrication of silicon based micro- and nano-cantilevers are most commonly fabricated using a well -established top down approach comprising of four main techniques; film deposition; photolithography; etching and doping [167]. An important consideration is the design and shape of the cantilever sensors, and the way such sensors can be combined into a micro-array. For optical detection schemes both rectangular and T shaped cantilevers are commonly employed [168], whilst capacitive detection systems benefit from square pads leading to increased sensitivity [169]. On the other hand piezoresistive cantilevers are designed U shaped with a partial Wheatstone bridge circuit. A recent report by Kermany *et al.*, (2014) fabricated microresonators with mechanical quality factors (Q) over a million using highly stressed epitaxial SiC on silicon wafers. Such high Q-factors were achieved using perfect-clamped string structure using silicon surface micromachining processes [170]. This study also demonstrated the use of two photolithography steps and as such two different masks followed by xenon difluoride dry etching to release the microbeams *(see figure 4)*. There is extensive debate for the selection of the best material for fabrication of microcantilever structures. With increased downscaling trends towards nanostructures, SiC has been realized as an ideal choice due to its ratio of Young's modulus (E) to mass density (ρ) is significantly higher than other semiconducting materials (Si, Si_3N_4, SiO_2, GaAs). Given the ratio $\sqrt{(E/\rho)}$ [124], SiC demonstrates high fundamental resonance frequencies, combined with small force constants enabling high sensitivity to realize the potential of NEMS. Additionally SiC's excellent chemical stability allows for surface treatments to achieve higher Q factors [170], [171]. This is vital as the NEMS Q factor is governed by surface defects [124], [172]. As discussed, 3C-SiC is an ideal polytype for fabricating complex resonators [4], [126], [129], [130], [166], [170], [173]. Yang *et al.,* (2001) fabricated nanometer scale single

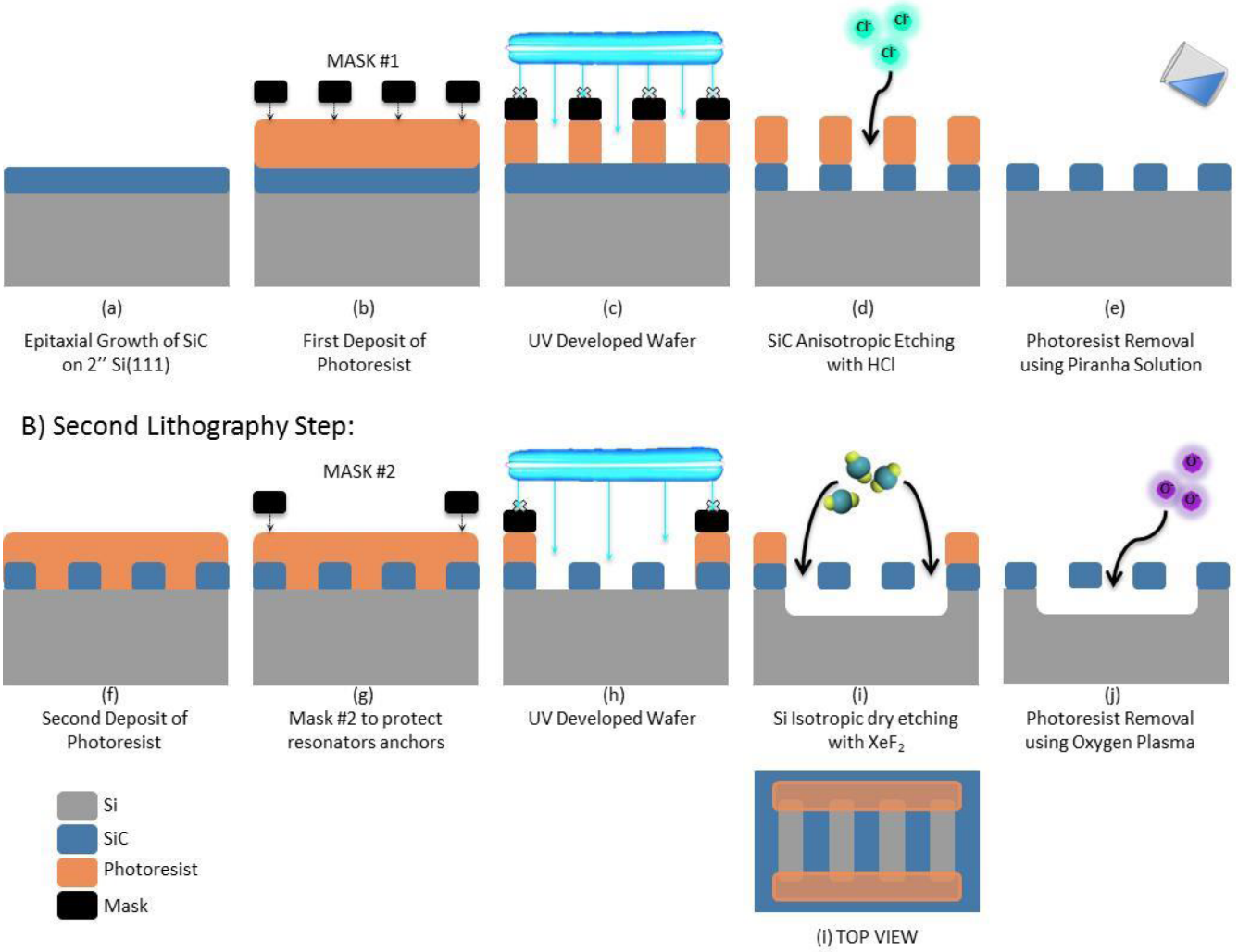

FIGURE 4. **Two lithography steps using preferential etching techniques to fabricate perfect clamped epitaxial SiC on Si microstrings. Adapted from [168].**

3C-SiC layers using dry etching to minimize damage caused by increased surface tension from wet etching. This study demonstrated that given the same geometry, nanometer-scale SiC resonators produce frequencies lower than GaAs and Si resonators [124]. Similarly increasing the residual stress of epitaxial 3C-SiC films enhances Q factors of SiC microstring resonators [170] outperforming the state-of-the-art based Si_3N_4 [174]. Si_3N_4 has long been the preferred resonator material, however, epitaxial 3C-SiC on silicon possesses additional advantages to this sensing platform. Unlike Si_3N_4, SiC is a semiconductor and thus can be doped [175], [176] and is piezoresistive [177]. Also note that sensors made of epitaxial 3C-SiC are expected to behave substantially better than poly-crystalline SiC sensors thanks to the absence of grain boundaries, and thus higher fracture resistance and resistance to corrosion. Finally, note that 3C-SiC is also a convenient alternative to Si_3N_4, as it can be used as solid source and template for direct transfer-free growth of graphene [178]–[180].

However, it is important to point out that at this stage, although the growth of 3C-SiC on silicon has seen substantial improvements, the interface of the SiC to the silicon substrate continues to be a problematic point. Additionally to being extremely defective because of the large mismatch stresses, it is also thermally unstable [F.Iacopi, unpublished data], which may prove an important limitation for some of the MEMS applications.

IV. GRAPHENE

Graphene is a one atom thick planar sheet of sp^2 bonded carbon atoms packed as a dense honeycomb crystal lattice with C-C bond length of 0.142 nm [181]. First isolated in 2004, through micromechanical cleavage of graphite [182]; graphene has revolutionized the nanotechnology platform as a next generation electronic sensing material. Monolayers and bilayers of graphene are zero-gap semiconductors; with only one electron charge carrier. With additional layers, several more charge carriers form, and as such the term

graphene has been limited to 10 layers before being considered graphite. Graphene has generated considerable attention due to its, anomalous quantum Hall effect [183], [184], absence of localization [185], chemical inertness [186], high thermal conductivity (5000 $Wm^{-1}K^{-1}$) [187], high current density [188], [189], optical transmittance [190], [191], super hydrophobicity at a nanometer scale [192], high electron mobility at room temperature (250,000 cm^2/Vs) [190], [193] and extraordinary mechanical properties with Young's modulus above 1 TPa [182], [194]. Additionally, reducing the dimensions of graphene to narrow ribbons the width of 1-2 nm, a distinct band gap can be attained, producing semiconductive graphene with unparalleled applications in transistors for nanoelectronics and high frequency applications [195], [196]. Graphene has been established as an outstanding conductor and plasmonic material. These properties allow for the augmentation of both MEMS and plasmonics label free methods as well as providing framework for further downscaling towards nanosensing devices.

A. BIOCOMPATIBILITY OF GRAPHENE

The remarkable properties of graphene have stimulated increased investigations into its biocompatibility due to broad prospective applications in biomedical engineering and biotechnology. Graphene-based materials (GBMs) biocompatibility relies on their intrinsic physical-chemical properties, which alter due to the raw materials and fabrication methods, used [197], [198]. Liao *et al.,* (2011) attributed cytotoxicity to the particle size, quality, state, surface charge and oxygen threshold. It was concluded that GBMs are capable of inducing superoxide anion-independent oxidative stress on bacterial cells through oxidation of (γ)-L-glutamyl-L-cysteinyl-glycine [199]. In a study by Liu *et al.,* (2011) the toxicity effect of four GBMs (graphite (Gt), graphite oxide (GtO), graphene oxide (GO) and reduced graphene oxide (rGO)) was investigated against *E. coli*. Oxidative stress signals revealed GO had the highest antibacterial activities (>rGO>Gt>GtO) [200]. Such investigations have led to the antimicrobial applications of graphene.

Biofilm formation on conducting materials in the long-term use of bioimplants and biosensors is a significant problem [201]. Advancements in antimicrobial graphene film coating provides a prospective alternative to previously explored surface coatings such as antibiotics [202] and cationic peptides [203]. A report by Santos *et al.,* compared the *E. coli* growth rates on GO with graphene-poly-*N*-vinyl carbazole (PVK) nanocomposites. Results indicate greater than a 80% microbial inhibition from PVK treatment of GO due to an increase in solution dispersion and as such increased interaction with the bacteria [204]. A similar study by Carpio *et al.,* (2012) using PVK-GO nanocomposites revealed a strong antimicrobial effect to both gram negative and positive bacteria. Additional testing against fibroblast cells (NIH 3T3) revealed a significant neutral toxicity leading to numerous potential biomedical applications for the prevention of biofilm formation [205].

Other applications using manganese-ferrite ($MnFe_2O_4$) decorated GO nanocomposites have been shown to be ideal as T_2 contrast MRI agents and use in magnetic hyperthermia for cancer therapy. Further PEGylation of these composites demonstrated exceptional biocompatibility [206]. Recent studies by Lee *et al.,* explore graphene-based tissue engineering approaches using various types of stem cells to restore damaged or lost tissues. Here, graphene's aromatic scaffold and good biocompatibility provides support for stem cell growth and differentiation through non-covalent binding [192], [207].

B. FABRICATION OF GRAPHENE

Several fabrication methods have been developed to produce graphene in large quantities the most common including micromechanical exfoliation of highly orientated pyrolytic graphite (HOPG) [182], CVD [208]–[210], Plasma enhanced CVD [211], [212] chemical reduction of graphite oxide (GO) [213], [214], CNTs unzipping [215]–[218] and epitaxial growth on bulk SiC [178]–[180], [219], [220]. Mechanical exfoliation is simple in principle, relying on separation of layers of stacked graphene sheets from graphite to produce individual sheets. Novoselov *et al.,* (2004) subjected a 1 mm thick HOPG sheet to dry etching in oxygen plasma to make multiple 5 μm deep plateaus. These were baked on a photoresist and subsequent peeled using scotch tape to remove layers from the graphite sheet. The resulting thin flakes were released from the photoresist in acetone and transferred to a Si substrate to yield mono to few-layer graphene sheets [182]. Though this first fabrication of graphene was indeed an exciting discovery, it is limited in its control over the number of layers produced and inability for large-scale production.

Accordingly, Stankovich *et al.,* (2007) proposed liquid phase exfoliation of graphite oxide due to its hydrophobicity for the large-scale production of graphene. This was achieved through exfoliation of GO nanosheets by ultrasonication in aqueous suspension and the subsequent reduction of these film in hydrazine hydrate at 100 °C for 24 hr [213]. However, Raman spectroscopic studies indicated that the invasive chemical treatment generated structural defects that disrupted the electronic structure of graphene [221]. It was later shown through XPS studies that even after chemical reduction or thermal annealing (up to 1000 °C), it is essentially impossible to regenerate the graphene structures [222].

To realize the promise for mass scale production of graphene, CVD approaches on metal surfaces provided a novel synthesis route for mono or few-layer graphene films. Somani *et al.,* (2006) first reported a thermal CVD (700-850 °C) technique to synthesize graphene from camphor on Ni foils. After cooling to ambient temperature yielded planar few layer graphene, high resolution transmission electron microscopy identified multiple folds and estimated to consist of 35 layers of graphene [210]. Whilst this method provides high quality graphene layers without complicated mechanical or chemical treatments, it still

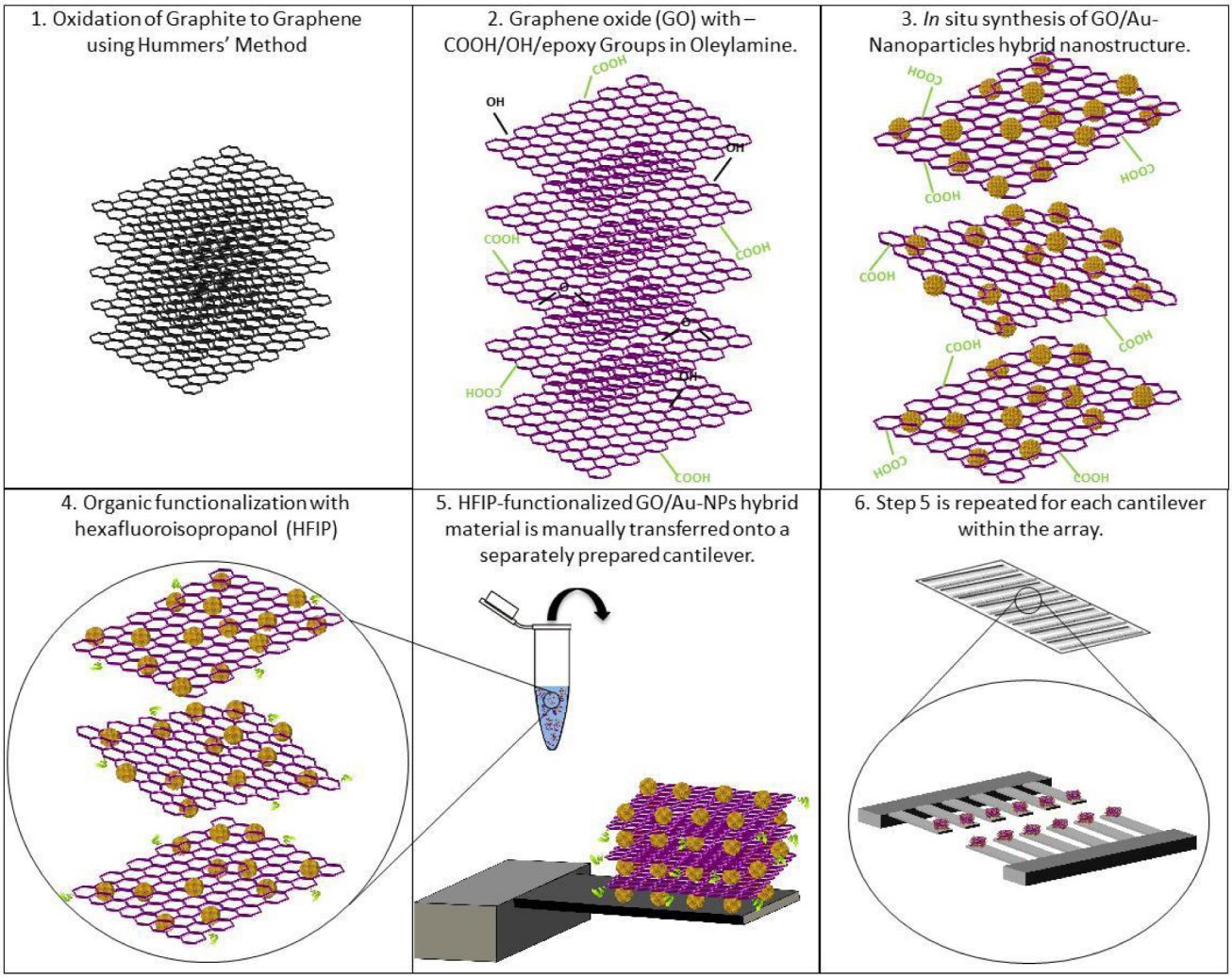

FIGURE 5. Gold (Au) – Nanoparticles (NP) *in situ* grown on bulk GO sheets to form GO/Au-NPs. Subsequent functionalization with hexafluoroisopropanol generates HFIP-functionalized GO/Au-NPs hybrid nanostructure suspensions that can be deposited onto pre-prepared cantilevers using a micromanipulator. Adapted from [229].

requires purification processes to eliminate the catalyst artifacts and transfer of graphene to another substrate. More recently, methods of transferring graphene using a micromanipulator and scanning electron microscope allow generation of GO nanoparticles that can be functionalized and used as biosensors. Xu *et al.,* (2013) demonstrated detection of trinitrotoluene (TNT) in 20 ppt using resonant microcantilever sensors functionalized with GO/Au nanoparticles (NP). The Au-NP serve as nanopillars to space GO sheets allowing molecules to access the nanopores. Hexafluoroisopropanol (HFIP) functionalized GO/Au-NPs hybrid material can be added to water to form a crude suspension, which can be loaded onto pre-prepared microcantilevers using a micromanipulator [229] *(see figure 5)*. However, transfer of graphene material requires precise manual handling techniques through the use of the micromanipulator and visualization with scanning electron microscopy (SEM) equipment, which can be expensive for smaller laboratories. Additionally, this method is effort- intensive, requiring serial functionalization of thousands of single cantilevers.

As stated graphene has a zero band gap and thus relies on introducing an energy band gap to be suitable for applications in semiconductors. This can be realized through either controlled oxidation of a few layers of graphene or fabrication of graphene nano ribbons (GNR). GNRs possess band gaps suitable for room temperature transistor operations with high carrier mobility due to narrow widths ($<$10 nm) and atomically smooth edges [217], [223], [224]. GNRs can be easily produced through e-beam lithography but this approach is limited by poor scale resolution (width of 20 nm) and large edge roughness [218], [225]–[227]. Accordingly, Jiao *et al.,* (2009) devised a novel approach through controlled unzipping of CNTs by argon plasma etching. This technique recognizes that CNTs are essentially GNRs rolled up into seamless tubes and therefore graphene growth can be controlled through the growth of CNTs. Multiwalled carbon nanotubes (MWCNTs) were embedded onto a poly (methyl

methacrylate) (PMMA) layer on a Si substrate. This PMMA etch mask was purpose designed to leave a narrow strip of MWCNT sidewall exposed to facilitate faster etching. Subsequent argon plasma treatment lead to unzipped CNTs and smooth edged GNRs with uniform width of 10-20 nm corresponding to half the circumference of the starting MWCNT [217]. Various new unzipping technique have emerged facilitating large scale production GNRs with controlled structure; however, it is important to note that these materials have inferior electronic characteristics when compared to wide peeled sheets of graphene [181], [228].

These fabrication methods to synthesize monolayer graphene and harness the extraordinary physical, optical, electronic and mechanical properties in actual micro- and nano-devices unfortunately still presents obstacles in the replication of well-defined structures when using transferred graphene [230], [231]. Precisely defined positions and dimensions is a requirement for the integration of graphene in MEMS and NEMS. Many methods reviewed require manipulation of exfoliated or grown graphene flakes and therefore are not considered suitable for augmenting such nanostructures. Encouragingly, a promising synthesis of homogenous, wafer size graphene for such technologies has been demonstrated by thermal decomposition of SiC [232]–[234].

C. GRAPHENE FROM SILICON CARBIDE

Interestingly, silicon carbide is a suitable template as well as solid-source for the direct (transfer –free) growth of graphene on semiconductor wafers. As such, silicon carbide bulk substrates are an ideal platform for the synthesis of graphene for micro and nanodevices. Investigation into graphitization by annealing of SiC surfaces in ultrahigh vacuum began in 1975 [235]. Unfortunately the process was limited in scale and very expensive. More recently graphene coated structures from epitaxial SiC films on Si has been realized as promising templates to augment MEMS and NEMS applications. SiC is advantageous due to already established photolithography and etching patterning [178], coupled to solid carbon source processes for graphene growth [233], [236]–[238]. The use of established self-aligned approaches facilitates exacting dimensions within the nanometer range for well-defined graphitized structures. Rollings *et al.,* (2006) reported successful growth of single crystalline mono to few layer graphene films from thermal decomposition (1200 °C) of the (0001) Si face of the 6H-SiC wafer [236]. Growth of epitaxial graphene by *in vacuo* silicon sublimation from the (0001) and (000-1) faces of 4H- and 6H-SiC has also been shown [228]. Various reports have characterized similar graphene growth on SiC through high temperature annealing in vacuum methods [239]–[241], however this has been recently shown to yield graphene layers with small grains (30–200 nm) [242], [243].

To address this, a report by Emtsev *et al.,* (2009) introduced a different approach of *ex situ* graphitization of (0001) Si face of 6H SiC in an argon atmosphere of 1 bar. Raman spectroscopy and Hall measurements of these large-size monolayer graphene films demonstrated improved quality of film with high electronic motilities ($\mu = 2{,}000\ \mathrm{cm}^2\ \mathrm{V}^{-1}\ \mathrm{s}^{-1}$ at $T = 27$ K) [242]. Nickel-mediated catalytic graphitization at the SiC surface to obtain graphene has emerged as a possible route. The catalytic action of Ni is vital as it reacts with SiC at comparably low temperature forming $NiSi_4$ to mediate the release of carbon required for the synthesis of graphene [178], [234], [244], [245]. Juang *et al.,* (2009) demonstrated low temperature (750 °C) synthesis of graphene on thin Ni films coated SiC substrates [237].

1) GRAPHITIZATION OF 3C-SiC

Graphitization of 3C-SiC on silicon is clearly a long sought-after goal, although it has historically been much more challenging. This is due to the lesser quality of the hetero-epitaxial SiC films on silicon, and the limitation of the graphene growth temperature to well below 1400 °C to remain within safe limits from the melting temperature of the silicon substrate. A suitable surface considered is 3C-SiC (111) as its top four layers are identical to those of 6H-SiC (0001), nevertheless challenges still arise from the high defects density of the hetero-epitaxial films due to the considerable lattice and thermal mismatch of Si and 3C- SiC [171], [246]. Many studies have demonstrated ultrathin graphene (monolayer, bilayer or multilayer) sheets from graphitization of 3C-SiC epilayers [247], [248] without needing to transfer the material to another insulating substrate before integration into MEMS and NEMS devices [249]. Finally graphitization of 3C-SiC (111) maintains a similar crystallographic structure that naturally accommodates the six-fold symmetry [250].

Investigations into reconstructions that lead to graphene growth have identified differences for the Si-terminated and C-terminated faces of SiC. On Si-terminated face scanning tunneling microscopy (STM) imagery has revealed a ''zeroth layer graphene'' as a $(6\sqrt{3} \times 6\sqrt{3})$R30° reconstructed interface layer that serves as a precursor stage of graphitization [251]. As such monolayer graphene is the first layer growing on top of this buffer layer, due to desorption of Si atoms [179], [252], [253] (*see figure 6)*. Epitaxial graphene annealed at temperatures larger than 900 - 1200 °C under Si flux induce gradual development of (3×3), (6×6), $(\sqrt{3}\times\sqrt{3})$ R30° and finally the reconstructed interface $(6\sqrt{3} \times 6\sqrt{3})$ R30° layer. A count of carbon atoms demonstrates that three SiC bilayers provide the carbon source for one graphene layer. Therefore it has been assumed that reformation of $(6\sqrt{3} \times 6\sqrt{3})$R30° reconstructed interface is required for each new graphene layer [254]. In this model the previous $(6\sqrt{3} \times 6\sqrt{3})$ R30° interface is released from its covalent bonding forming the next graphene layer. This interface ensures the same 30° rotation for all graphene layers grown on the SiC substrate.

Alternatively, on the C-terminated face the $(6\sqrt{3} \times 6\sqrt{3})$ R30° reconstruction is not observed, and the atomic transformation of graphene not as easily clarified. Studies by Gupta *et al.,* using XPS, STM and Raman spec-

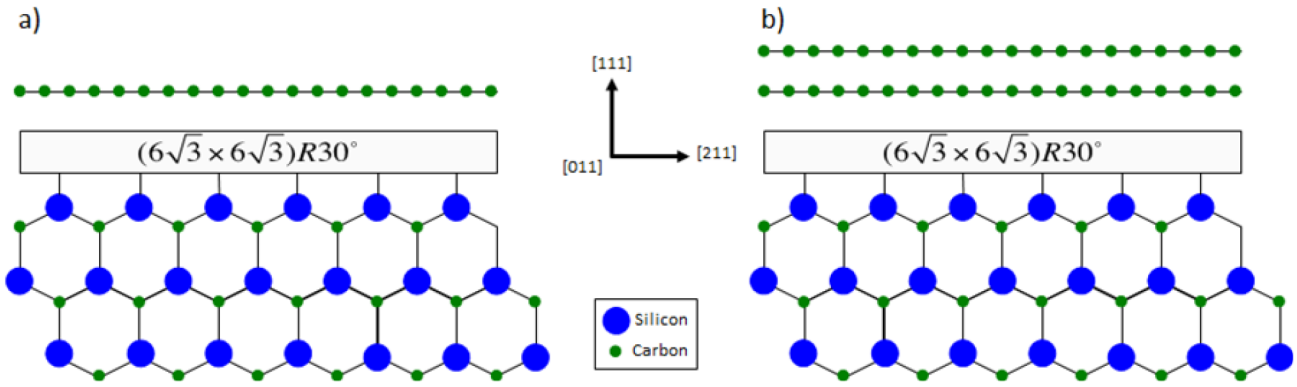

FIGURE 6. Cross sectional structural model along the [011] cubic SiC zone axis of (a) monolayer and (b) bilayer epitaxial graphene on 3C- SiC(111). The graphene is growing on top of the (6√3 × 6√3)R30° reconstructed interface layer.

troscopy reveal interesting details on the transformation from 3C SiC (111)/Si (111) to graphene at different temperatures (1125 to 1375 °C). STM imaging revealed continuous hexagonal structure mono to few-layer graphene (1 × 1) with hole-to-hole dimensions of 0.246 nm. Images also demonstrate transition from 3C SiC (111)/Si (111) to graphene at 1250 °C occurred in two subsequent steps: transition from SiC surface $(\sqrt{3}\times\sqrt{3})$ R30° to $(\frac{3}{2}\times\sqrt{3})$ R30° followed by monolayer graphene. Wrinkled areas were attributed to defects in the underlying SiC/Si (111) and remain an issue of lattice mismatch. Raman spectroscopy indicates that G band shifts towards lower wavelengths, and as such an increase in graphene layer thickness is a strong function of increases in annealing temperature [179], [180]. Finally this investigation noted that 3C-SiC does not depict second order Raman features between 1450 and 1750 cm^{-1} as in other polytypes of SiC [255].

Synthesis of graphene on epitaxial SiC on Si (briefly discussed earlier) by Cunning *et al.*, (2014) demonstrate uniform and high- quality graphene synthesis using a Ni-Cu alloy catalyst. A pre-patterned 3C-SiC layer (250 nm) on a Si (111) wafer was sputtered with nickel and copper. Subsequent site selective graphitization at 1000 °C through; (a) Kirkendall diffusion of the nickel and copper; (b) silicide formation to generate a carbon source for graphitization; (c) removal of intermixed metal to expose the graphene on the SiC through

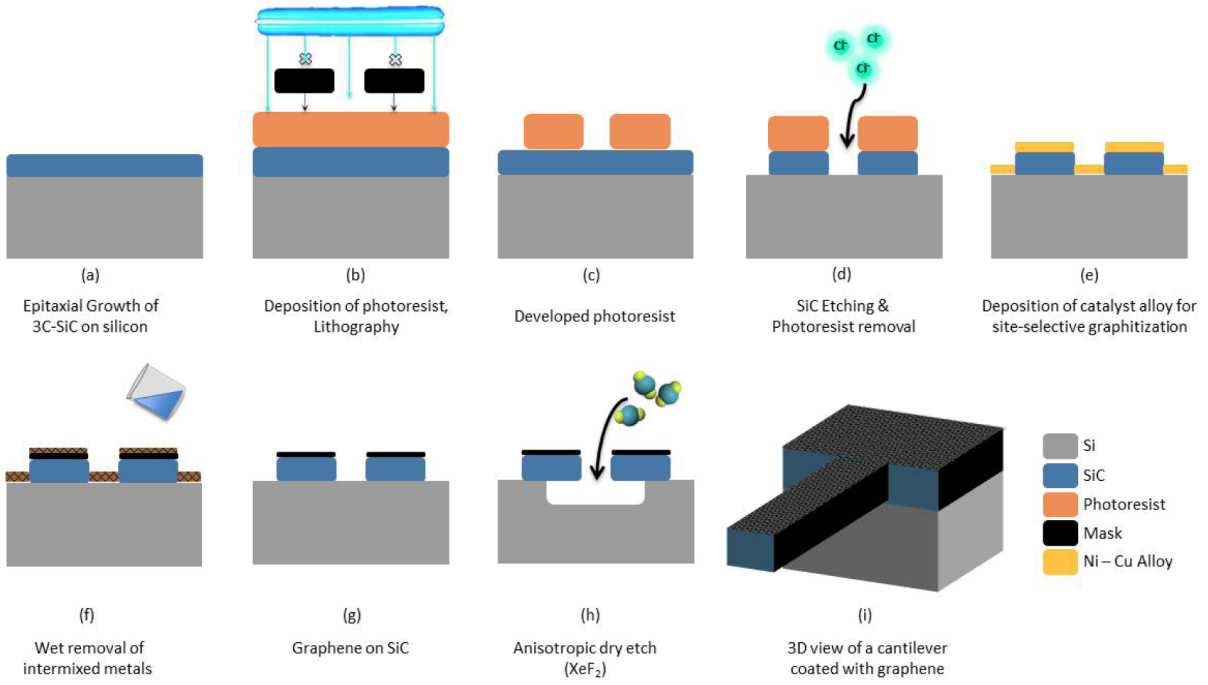

FIGURE 7. Wafer-level fabrication of graphitized silicon carbide microbeams on a silicon substrate. The SiC can be patterned to generate thousands of cantilevers and thus removes the need for manipulation of single flakes. The few-layer graphene is grown selectively on the SiC structures via site-selected graphitization. Adapted from [176].

sonication in a Freckle's etch solution [178] *(see figure 7)*. This self-aligned nanocoating of few layer graphene onto suspended SiC microstructures is ideal for replacing current conducting layer in MEMS, as well as providing alternate surface functionalization routes. This novel synthesis approach is also advantageous as it can be performed at temperatures compatible with conventional semiconductor processing, allowing complex device integration and generation of thousands of MEMS/NEMS by pre-patterning of the SiC. A follow up study by Iacopi *et al.,* (2015) introduced novel synthesis of high quality and highly uniform few layer graphene from epitaxial 3C-SiC films on Si (100) and Si (111) using the described [178] Ni/Cu catalytic alloy approach. Transmission electron microscopy in this study [232] yielded <0.9 nm thin bilayer graphene with high-quality and high adhesion to the substrate [256]. Such advances open enormous new opportunities for harnessing the properties of graphene for MEMS and NEMS devices fabricated at the wafer -level.

D. FUNCTIONALIZATION OF GRAPHENE

Graphene can be prepared readily through chemical, thermal or photo-chemical reduction of GO, and this is the type of graphene most heavily investigated so far for functionalisation. However, subsequent graphene formation can lead to precipitation of graphite particles and sheet aggregation due to lack of a stabilizer [257]. As such covalent or non-covalent surface functionalization is performed before reducing the graphene sheets [258]. Fortunately this process enables the immobilization of biomolecules through surface functionalization of highly oxygenated GO sheets. Covalent functionalization of this framework occurs through hybridization of one or more sp^2 carbon atoms into the sp^3 configuration [259] through either nucleophilic substitution [260], [261] electrophilic addition [262], [263], condensation reactions [264], [265] or addition reactions [266], [267].

Nucleophilic substitution reactions are commonly employed for the functionalization of GO as it occurs easily at room temperature and in an aqueous medium. Organic modifiers containing the amine functionality can undergo nucleophilic substitution reactions that target the epoxy groups of GO. Many aliphatic and aromatic amines, amino acids, amine-terminated biomolecules and small molecular weight polymers have been successfully prepared on functionalized graphene [257]. For example, Kuila *et al* (2010) used dodecyl amine (DA) and octadecyl amine (ODA) for the surface treatment of graphene, [268] the results being similar to those of Bourlinos *et al*., (2003) who demonstrated that amine intercalated GO derivatives depend on amine chain length [261]. Chemical functionalization of graphene sheets can also be carried out with APTES [260]. Similar APTES chemistry has previously been described on SiC platforms and as such could provide a suitable framework to integrate graphene into MEMS systems. A study by Shan *et al*., (2009) generated biocompatible graphene functionalized with poly-L-lysine (PLL) to immobilize biomolecules. The resulting biosensor was conjugated to horseradish peroxide (HRP) to create graphene-PLL/HRP nanocomposites capable of sensing H_2O_2 [269]. Graphene functionalization through condensation reactions has been shown to occur through loss of entropy. Recent investigations have demonstrated that condensation occurs with isocyanate, diisocyanate, and amine compounds through the formation of amides and carbonate ester linkages. Stankovich *et al*., (2006) functionalized graphene using isocyanate compounds revealed reduced hydrophilic properties, which through further exfoliation yielded derivatized, GO nanoplatelets [264]. Diisocyantes have also been used for graphene functionalization by activating the carboxyl functionality using thionyl chloride ($SOCl_2$). This nanoporous material displayed promise as a hydrogen adsorbent material [270]. Finally, Liu *et al.,* (2008) first reported GO functionalization using poly(ethylene glycol) ($PEG\text{-}NH_2$) through a carbodiimide catalyzed amide formation. Various insoluble aromatic drug molecules such as camptothecin analogues and Iressa (Gefitinib) were successfully loaded onto nanoscale graphene oxide-PEG via simple adsorption [265], [271]. Further studies to optimize functionalization of graphene for biomolecule immobilization highlights a promising pathway for increased sensitivity and NEMS downscaling.

V. CONCLUSION

Label free, analyte specific, accurate, and highly sensitive biochemical detection systems will offer superior capabilities over existing systems in terms of high-throughput, efficient drug screening and early pathogen detection. Research in this area, underpinned by novel functional (nano)materials, is now reaching maturity and offers perspectives of concrete advances. Silicon carbide, potentially combined with transfer –free graphene, is one prominent example of material system that could provide enormous advances, either through plasmonics or micro-electro-mechanical systems. Additionally, the possibility for scaling down the sizes of such sensors towards the nanoscale, together with ensuring the bio- and hemo-compatibility of the materials involved, could potentially enable minimally invasive endoscopic detection, with enormous benefits for early detection of life-threatening diseases such as cancer.

ACKNOWLEDGMENT

O.C thanks Atieh R. Kermany and Neeraj Mishra for their invaluable input and guidance throughout the preparation of this manuscript.

REFERENCES

[1] P. M. Sarro, "Silicon carbide as a new MEMS technology," *Sens. Actuators A, Phys.*, vol. 82, nos. 1–3, pp. 210–218, May 2000.
[2] A. L. Spetz *et al.*, "New materials for chemical and biosensors," *Mater. Manuf. Process.*, vol. 21, no. 3, pp. 253–256, May 2006.
[3] F. Iacopi, M. Van Hove, M. Charles, and K. Endo, "Power electronics with wide bandgap materials: Toward greener, more efficient technologies," *MRS Bull.*, vol. 40, no. 5, pp. 390–395, 2015.
[4] C. L. Frewin, C. Locke, S. E. Saddow, and E. J. Weeber, "Single-crystal cubic silicon carbide: An *in vivo* biocompatible semiconductor for brain machine interface devices," in *Proc. Annu. Int. Conf. IEEE Eng. Med. Biol. Soc.*, Aug./Sep. 2011, pp. 2957–2960.

[5] C. L. Frewin *et al.*, "Atomic force microscopy analysis of central nervous system cell morphology on silicon carbide and diamond substrates," *J. Molecular Recognit.*, vol. 22, no. 5, pp. 380–388, 2009.

[6] S. E. Saddow, C. L. Coletti, C. Frewin, N. C. Schettini, A. Oliveros, and M. Jaroszeski, "Single-crystal silicon carbide: A biocompatible and hemocompatible semiconductor for advanced biomedical applications," *Proc. MRS Symp.*, vol. 679, pp. 824–830, Feb. 2011.

[7] C. Coletti, M. J. Jaroszeski, A. Pallaoro, A. M. Hoff, S. Iannotta, and S. E. Saddow, "Biocompatibility and wettability of crystalline SiC and Si surfaces," in *Proc. 29th Annu. Int. Conf. IEEE Eng. Med. Biol. Soc.*, Aug. 2007, pp. 5849–5852.

[8] C. L. Frewin *et al.*, "The development of silicon carbide based electrode devices for central nervous system biomedical implants," in *Proc. MRS Symp.*, vol. 1236, pp. 1236-SS01-02, Jan. 2011.

[9] S. Saddow, Eds., *Silicon Carbide Biotechnology: A Biocompatible Semiconductor for Advanced Biomedical Devices and Applications*. Amsterdam, The Netherlands: Elsevier, 2011.

[10] S. Dai *et al.*, "Graphene on hexagonal boron nitride as a tunable hyperbolic metamaterial," *Nature Nanotechnol.*, vol. 10, no. 8, pp. 682–686, Aug. 2015.

[11] J. T. Kemp, R. W. Davis, R. L. White, S. X. Wang, and C. D. Webb, "A novel method for STR-based DNA profiling using microarrays," *J. Forensic Sci.*, vol. 50, no. 5, pp. 1109–1113, Sep. 2005.

[12] C. P. Paweletz *et al.*, "Reverse phase protein microarrays which capture disease progression show activation of pro-survival pathways at the cancer invasion front," *Oncogene*, vol. 20, no. 16, pp. 1981–1989, Apr. 2001.

[13] S. Nishizuka *et al.*, "Proteomic profiling of the NCI-60 cancer cell lines using new high-density reverse-phase lysate microarrays," *Proc. Nat. Acad. Sci. USA*, vol. 100, no. 24, pp. 14229–14234, Nov. 2003.

[14] C. J. Day, G. Tram, L. E. Hartley-Tassell, J. Tiralongo, and V. Korolik, "Assessment of glycan interactions of clinical and avian isolates of *Campylobacter jejuni*," *BMC Microbiol.*, vol. 13, no. 1, p. 1, Oct. 2013.

[15] P.-H. Liang, C.-Y. Wu, W. A. Greenberg, and C.-H. Wong, "Glycan arrays: Biological and medical applications," *Curr. Opin. Chem. Biol.*, vol. 12, no. 1, pp. 86–92, Dec. 2007.

[16] N. X. Arndt *et al.*, "Differential carbohydrate binding and cell surface glycosylation of human cancer cell lines," *J. Cell. Biochem.*, vol. 112, no. 9, pp. 2230–2240, Aug. 2011.

[17] S. C. Tao *et al.*, "Lectin microarrays identify cell-specific and functionally significant cell surface glycan markers," *Glycobiology*, vol. 18, no. 10, pp. 761–769, Sep. 2008.

[18] R. Akbani *et al.*, "Realizing the promise of reverse phase protein arrays for clinical, translational, and basic research: A workshop report: The RPPA (reverse phase protein array) society," *Molecular Cellular Proteomics*, vol. 13, no. 7, pp. 1625–1643, Jul. 2014.

[19] D. A. Hall, J. Ptacek, and M. Snyder, "Protein microarray technology," *Mech. Ageing Develop.*, vol. 128, no. 1, pp. 161–167, Jan. 2007.

[20] N. Ramachandran, D. N. Larson, P. R. H. Stark, E. Hainsworth, and J. LaBaer, "Emerging tools for real-time label-free detection of interactions on functional protein microarrays," *FEBS J.*, vol. 272, no. 21, pp. 5412–5425, Nov. 2005.

[21] K. A. Willets and R. P. Van Duyne, "Localized surface plasmon resonance spectroscopy and sensing," *Annu. Rev. Phys. Chem.*, vol. 58, pp. 267–297, May 2007.

[22] A. Otto, "Excitation of nonradiative surface plasma waves in silver by the method of frustrated total reflection," *Zeitschrift Phys.*, vol. 216, pp. 398–410, Aug. 1968.

[23] J. Homola, "Surface plasmon resonance sensors for detection of chemical and biological species," *Chem. Rev.*, vol. 108, no. 2, pp. 462–493, Feb. 2008.

[24] J. Homola, S. S. Yee, and G. Gauglitz, "Surface plasmon resonance sensors: Review," *Sens. Actuators B, Chem.*, vol. 54, no. 1, pp. 3–15, Dec. 1998.

[25] I. Choi and Y. Choi, "Plasmonic nanosensors: Review and prospect," *IEEE J. Sel. Topics Quantum Electron.*, vol. 18, no. 3, pp. 1110–1121, May/Jun. 2012.

[26] J. G. Gordon, II, and S. Ernst, "Surface plasmons as a probe of the electrochemical interface," *Surf. Sci.*, vol. 101, nos. 1–3, pp. 499–506, Jan. 1980.

[27] S. M. Tabakman *et al.*, "Plasmonic substrates for multiplexed protein microarrays with femtomolar sensitivity and broad dynamic range," *Nature Commun.*, vol. 2, p. 466, Sep. 2011.

[28] J. N. Anker, W. P. Hall, O. Lyandres, N. C. Shah, J. Zhao, and R. P. Van Duyne, "Biosensing with plasmonic nanosensors," *Nature Mater.*, vol. 7, no. 6, pp. 442–453, May 2008.

[29] A. G. Brolo, R. Gordon, B. Leathem, and K. L. Kavanagh, "Surface plasmon sensor based on the enhanced light transmission through arrays of nanoholes in gold films," *Langmuir*, vol. 20, no. 12, pp. 4813–4815, Jun. 2004.

[30] T. Kang, J. Moon, S. Oh, S. Hong, S. Chah, and J. Yi, "Direct observation of a cooperative mechanism in the adsorption of heavy metal ions to thiolated surface by in-situ surface plasmon resonance measurements," *Chem. Commun.*, no. 18, vol. 18, pp. 2360–2362, May 2005.

[31] H. Im, A. Lesuffleur, N. C. Lindquist, and S.-H. Oh, "Plasmonic nanoholes in a multichannel microarray format for parallel kinetic assays and differential sensing," *Anal. Chem.*, vol. 81, no. 8, pp. 2854–2859, 2009.

[32] C. R. Yonzon, E. Jeoung, S. Zou, G. C. Schatz, M. Mrksich, and R. P. Van Duyne, "A comparative analysis of localized and propagating surface plasmon resonance sensors: The binding of concanavalin a to a monosaccharide functionalized self-assembled monolayer," *J. Amer. Chem. Soc.*, vol. 126, no. 39, pp. 12669–12676, Oct. 2004.

[33] T. Kang, S. Oh, S. Hong, J. Moon, and J. Yi, "Mesoporous silica thin films as a spatially extended probe of interfacial electric fields for amplified signal transduction in surface plasmon resonance spectroscopy," *Chem. Commun.*, no. 28, vol. 28, pp. 2998–3000, Jul. 2006.

[34] T. R. Jensen, M. D. Malinsky, C. L. Haynes, and R. P. Van Duyne, "Nanosphere lithography: Tunable localized surface plasmon resonance spectra of silver nanoparticles," *J. Phys. Chem. B*, vol. 104, no. 45, pp. 10549–10556, Nov. 2000.

[35] T. Kang *et al.*, "Reversible pH-driven conformational switching of tethered superoxide dismutase with gold nanoparticle enhanced surface plasmon resonance spectroscopy," *J. Amer. Chem. Soc.*, vol. 128, no. 39, pp. 12870–12878, Oct. 2006.

[36] P. L. Stiles, J. A. Dieringer, N. C. Shah, and R. P. Van Duyne, "Surface-enhanced Raman spectroscopy," *Annu. Rev. Anal. Chem.*, vol. 1, no. 1, pp. 601–626, Jul. 2008.

[37] A. J. Haes, S. Zou, G. C. Schatz, and R. P. Van Duyne, "A nanoscale optical biosensor: The long range distance dependence of the localized surface plasmon resonance of noble metal nanoparticles," *J. Phys. Chem. B*, vol. 108, no. 1, pp. 109–116, 2004.

[38] A. D. McFarland, M. A. Young, J. A. Dieringer, and R. P. Van Duyne, "Wavelength-scanned surface-enhanced Raman excitation spectroscopy," *J. Phys. Chem. B*, vol. 109, no. 22, pp. 11279–11285, Jun. 2005.

[39] R. Karlsson, "SPR for molecular interaction analysis: A review of emerging application areas," *J. Molecular Recognit.*, vol. 17, no. 3, pp. 151–161, May/Jun. 2004.

[40] V. Kanda, J. K. Kariuki, D. J. Harrison, and M. T. McDermott, "Label-free reading of microarray-based immunoassays with surface plasmon resonance imaging," *Anal. Chem.*, vol. 76, no. 24, pp. 7257–7262, Dec. 2004.

[41] J. S. Yuk *et al.*, "Analysis of protein interactions on protein arrays by a novel spectral surface plasmon resonance imaging," *Biosensors Bioelectron.*, vol. 21, no. 8, pp. 1521–1528, 2006.

[42] M. Medina-Sánchez, S. Miserere, and A. Merkoçi, "Nanomaterials and lab-on-a-chip technologies," *Lab Chip*, vol. 12, no. 11, pp. 1932–1943, May 2012.

[43] A. V. Whitney *et al.*, "Localized surface plasmon resonance nanosensor: A high-resolution distance-dependence study using atomic layer deposition," *J. Phys. Chem. B*, vol. 109, no. 43, pp. 20522–20528, Nov. 2005.

[44] S. Kim, J.-M. Jung, D.-G. Choi, H.-T. Jung, and S.-M. Yang, "Patterned arrays of Au rings for localized surface plasmon resonance," *Langmuir*, vol. 22, no. 17, pp. 7109–7112, 2006.

[45] E. M. Larsson, J. Alegret, M. Käll, and D. S. Sutherland, "Sensing characteristics of NIR localized surface plasmon resonances in gold nanorings for application as ultrasensitive biosensors," *Nano Lett.*, vol. 7, no. 5, pp. 1256–1263, Apr. 2007.

[46] L. A. Dick, A. J. Haes, and R. P. Van Duyne, "Distance and orientation dependence of heterogeneous electron transfer: A surface-enhanced resonance Raman scattering study of cytochrome c bound to carboxylic acid terminated alkanethiols adsorbed on silver electrodes," *J. Phys. Chem. B*, vol. 104, no. 49, pp. 11752–11762, 2000.

[47] I. Ruach-Nir, T. A. Bendikov, I. Doron-Mor, Z. Barkay, A. Vaskevich, and I. Rubinstein, "Silica-stabilized gold island films for transmission localized surface plasmon sensing," *J. Amer. Chem. Soc.*, vol. 129, no. 1, pp. 84–92, Jan. 2007.
[48] P. S. Waggoner and H. G. Craighead, "Micro- and nanomechanical sensors for environmental, chemical, and biological detection," *Lab Chip*, vol. 7, no. 10, p. 1238, 2007.
[49] W. J. Choyke and G. Pensl, "Physical properties of SiC," *MRS Bull.*, vol. 22, no. 3, pp. 25–29, Mar. 1997.
[50] G. Wu, R. H. Datar, K. M. Hansen, T. Thundat, R. J. Cote, and A. Majumdar, "Bioassay of prostate-specific antigen (PSA) using micro-cantilevers," *Nature Biotechnol.*, vol. 19, no. 9, pp. 856–860, Aug. 2001.
[51] P. J. Hesketh, G. Barna, and H. G. Hughes, *Microstructures and Microfabricated Systems III*. Pennington, NJ, USA: ECS, 1997.
[52] J. Gamby, A. Rudolf, M. Abid, H. H. Girault, C. Deslouis, and B. Tribollet, "Polycarbonate microchannel network with carpet of gold nanowires as SERS-active device," *Lab Chip*, vol. 9, no. 12, pp. 1806–1808, Jun. 2009.
[53] P. R. West, S. Ishii, G. V. Naik, N. Emani, V. M. Shalaev, and A. Boltasseva, "Searching for better plasmonic materials," *Laser Photon. Rev.*, vol. 4, no. 6, pp. 795–808, Nov. 2009.
[54] M. G. Blaber, M. D. Arnold, and M. J. Ford, "Designing materials for plasmonic systems: The alkaliŰnoble intermetallics," *J. Phys., Condens. Matter*, vol. 22, no. 9, p. 095501, 2010.
[55] A. Boltasseva and H. A. Atwater, "Low-loss plasmonic metamaterials," *Mater. Sci.*, vol. 331, no. 6015, pp. 290–291, Jan. 2011.
[56] R.-M. Ma, R. F. Oulton, V. J. Sorger, and X. Zhang, "Plasmon lasers: Coherent light source at molecular scales," *Laser Photon. Rev.*, vol. 7, no. 1, pp. 1–21, Feb. 2012.
[57] H. Wei and H. Xu, "Plasmonics in composite nanostructures," *Biochem. Pharmacol.*, vol. 17, no. 8, pp. 372–380, Oct. 2014.
[58] O. J. Glembocki *et al.*, "Beyond electron based metamaterials: Low-loss surface phonon polariton-based nano-antenna arrays using silicon carbide," in *Proc. ECS Meeting Abstracts*, pp. 1548–1548, 2014.
[59] K. Brueckner *et al.*, "Micro- and nano-electromechanical resonators based on SiC and group III-nitrides for sensor applications," *Phys. Status Solidi A*, vol. 208, no. 2, pp. 357–376, Jul. 2010.
[60] M. L. Roukes, "Nanoelectromechanical systems," in *Tech. Digest 2000 Solid-State Sen. Actuat. Workshop, Hilton Head Island, SC*, pp. 1–10, 2000.
[61] P.-S. Lee *et al.*, "Microcantilevers with nanochannels," *Adv. Mater.*, vol. 20, no. 9, pp. 1732–1737, 2008.
[62] P. I. Oden, G. Y. Chen, R. A. Steele, R. J. Warmack, and T. Thundat, "Viscous drag measurements utilizing microfabricated cantilevers," *Appl. Phys. Lett.*, vol. 68, no. 26, pp. 3814–3816, 1996.
[63] G. Meyer and N. M. Amer, "Novel optical approach to atomic force microscopy," *Appl. Phys. Lett.*, vol. 53, no. 12, pp. 1045–1047, 1988.
[64] R. Datar *et al.*, "Cantilever sensors: Nanomechanical tools for diagnostics," *MRS Bull.*, vol. 34, no. 6, pp. 449–454, Jun. 2009.
[65] H. Ibach, "Adsorbate-induced surface stress," *J. Vac. Sci. Technol. A*, vol. 12, no. 4, p. 2240, 1994.
[66] T. Thundat, L. Pinnaduwage, and R. Lareau, "Explosive vapour detection using micromechanical sensors," *Abstr. Pap. Am. Chem. S.*, vol. 159, pp. 249–266, 2004.
[67] G. G. Stoney, "The tension of metallic films deposited by electrolysis," *Proc. Roy. Soc. London A*, vol. 82, no. 553, pp. 172–175, May 1909.
[68] K. S. Hwang, J. H. Lee, J. Park, D. S. Yoon, J. H. Park, and T. S. Kim, "In-situ quantitative analysis of a prostate-specific antigen (PSA) using a nanomechanical PZT cantilever," *Lab Chip*, vol. 4, no. 6, pp. 547–552, Nov. 2004.
[69] H. P. Lang, M. Hegner, and C. Gerber, "Nanomechanics—The link to biology and chemistry," *CHIMIA Int. J. Chem.*, vol. 56, no. 10, pp. 515–519, Oct. 2002.
[70] K. E. Petersen and C. R. Guarnieri, "Young's modulus measurements of thin films using micromechanics," *J. Appl. Phys.*, vol. 50, no. 11, p. 6761, 1979.
[71] K. M. Goeders, J. S. Colton, and L. A. Bottomley, "Microcantilevers: Sensing chemical interactions via mechanical motion," *Chem. Rev.*, vol. 108, no. 2, pp. 522–542, Feb. 2008.
[72] F. R. Blom, S. Bouwstra, M. Elwenspoek, and J. H. J. Fluitman, "Dependence of the quality factor of micromachined silicon beam resonators on pressure and geometry," *J. Vac. Sci. Technol. B*, vol. 10, no. 1, pp. 19–26, Jan. 1992.
[73] J. Tamayo, "Study of the noise of micromechanical oscillators under quality factor enhancement via driving force control," *J. Appl. Phys.*, vol. 97, no. 4, p. 044903, 2005.
[74] J. Fritz *et al.*, "Translating biomolecular recognition into nanomechanics," *Science*, vol. 288, no. 5464, pp. 316–318, Apr. 2000.
[75] B. Ilic, Y. Yang, K. Aubin, R. Reichenbach, S. Krylov, and H. G. Craighead, "Enumeration of DNA molecules bound to a nanomechanical oscillator," *Nano Lett.*, vol. 5, no. 5, pp. 925–929, Apr. 2005.
[76] A. Boisen, J. Thaysen, H. Jensenius, and O. Hansen, "Environmental sensors based on micromachined cantilevers with integrated read-out," *Ultramicroscopy*, vol. 82, nos. 1–4, pp. 11–16, Dec. 1999.
[77] R. Mukhopadhyay, M. Lorentzen, J. Kjems, and F. Besenbacher, "Nanomechanical sensing of DNA sequences using piezoresistive cantilevers," *Langmuir*, vol. 21, no. 18, pp. 8400–8408, Aug. 2005.
[78] K. W. Wee *et al.*, "Novel electrical detection of label-free disease marker proteins using piezoresistive self-sensing micro-cantilevers," *Biosensors Bioelectron.*, vol. 20, no. 10, pp. 1932–1938, Apr. 2005.
[79] G. Binnig, C. F. Quate, and C. Gerber, "Atomic force microscope," *Phys. Rev. Lett.*, vol. 56, no. 9, pp. 930–933, 1986.
[80] N. V. Lavrik, M. J. Sepaniak, and P. G. Datskos, "Cantilever transducers as a platform for chemical and biological sensors," *Rev. Sci. Instrum.*, vol. 75, no. 7, pp. 2229–2253, Jul. 2004.
[81] C. L. Britton, Jr., *et al.*, "Multiple-input microcantilever sensors," *Ultramicroscopy*, vol. 82, nos. 1–4, pp. 17–21, Feb. 2000.
[82] M. Zougagh and A. Ríos, "Micro-electromechanical sensors in the analytical field," *Analyst*, vol. 134, no. 7, pp. 1274–1290, 2009.
[83] K. M. Hansen *et al.*, "Cantilever-based optical deflection assay for discrimination of dna single-nucleotide mismatches," *Anal. Chem.*, vol. 73, no. 7, pp. 1567–1571, Apr. 2001.
[84] G. Stemme, "Resonant silicon sensors," *J. Micromech. Microeng.*, vol. 1, no. 2, pp. 113–125, Jun. 1991.
[85] P. A. Rasmussen, J. Thaysen, O. Hansen, S. C. Eriksen, and A. Boisen, "Optimised cantilever biosensor with piezoresistive read-out," *Ultramicroscopy*, vol. 97, nos. 1–4, pp. 371–376, Oct. 2003.
[86] G. A. Campbell and R. Mutharasan, "Piezoelectric-excited millimeter-sized cantilever (PEMC) sensors detect Bacillus anthracis at 300 spores/mL," *Biosensors Bioelectron.*, vol. 21, no. 9, pp. 1684–1692, Mar. 2006.
[87] G. Kotzar *et al.*, "Evaluation of MEMS materials of construction for implantable medical devices," *Biomaterials*, vol. 23, no. 13, pp. 2737–2750, Jun. 2002.
[88] S. S. Lee and R. M. White, "Self-excited piezoelectric cantilever oscillators," *Sens. Actuators A, Phys.*, vol. 52, nos. 1–3, pp. 41–45, Dec. 1995.
[89] J. H. Lee, K. H. Yoon, K. S. Hwang, J. Park, S. Ahn, and T. S. Kim, "Label free novel electrical detection using micromachined PZT monolithic thin film cantilever for the detection of C-reactive protein," *Biosensors Bioelectron.*, vol. 20, no. 2, pp. 269–275, Sep. 2004.
[90] R. S. Wagner and W. C. Ellis, *Vapor-Liquid-Solid Mechanism of Crystal Growth and Its Application to Silicon*. New York, NY, USA: AIME, 1965.
[91] L. Latu-Romain and M. Ollivier, "Silicon carbide based one-dimensional nanostructure growth: Towards electronics and biology perspectives," *J. Phys. D, Appl. Phys.*, vol. 47, no. 20, p. 203001, May 2014.
[92] S. A. Fortuna and X. Li, "TOPICAL REVIEW: Metal-catalyzed semiconductor nanowires: A review on the control of growth directions," *Semicond. Sci. Technol.*, vol. 25, no. 2, p. 024005, Feb. 2010.
[93] R. Rurali, "*Colloquium*: Structural, electronic, and transport properties of silicon nanowires," *Rev. Mod. Phys.*, vol. 82, no. 1, pp. 427–449, Jan. 2010.
[94] L. J. Lauhon, M. S. Gudiksen, D. Wang, and C. M. Lieber, "Epitaxial core–shell and core–multishell nanowire heterostructures," *Nature*, vol. 420, no. 6911, pp. 57–61, Nov. 2002.
[95] Y. Cui, Q. Wei, H. Park, and C. M. Lieber, "Nanowire nanosensors for highly sensitive and selective detection of biological and chemical species," *Science*, vol. 293, no. 5533, pp. 1289–1292, Aug. 2001.
[96] F. Patolsky, G. Zheng, O. Hayden, M. Lakadamyali, X. Zhuang, and C. M. Lieber, "Electrical detection of single viruses," *Proc. Nat. Acad. Sci. USA*, vol. 101, no. 39, pp. 14017–14022, Sep. 2004.
[97] X. Song, B. Xia, S. R. Stowell, Y. Lasanajak, D. F. Smith, and R. D. Cummings, "Novel fluorescent glycan microarray strategy reveals ligands for galectins," *Chem. Biol.*, vol. 16, no. 1, pp. 36–47, Jan. 2009.
[98] M. Safi *et al.*, "Interactions between magnetic nanowires and living cells: Uptake, toxicity, and degradation," *ACS Nano*, vol. 5, no. 7, pp. 5354–5364, Jul. 2011.

[99] S. Iijima, "Helical microtubules of graphitic carbon," *Nature*, vol. 354, pp. 56–58, Nov. 1991.

[100] J. Okuno, K. Maehashi, K. Kerman, Y. Takamura, K. Matsumoto, and E. Tamiya, "Label-free immunosensor for prostate-specific antigen based on single-walled carbon nanotube array-modified microelectrodes," *Biosensors Bioelectron.*, vol. 22, nos. 9–10, pp. 2377–2381, Apr. 2007.

[101] J.-C. Charlier, X. Blase, and S. Roche, "Electronic and transport properties of nanotubes," *Rev. Mod. Phys.*, vol. 79, no. 2, pp. 677–732, May 2007.

[102] S.-P. Huang *et al.*, "First-principles study: Size-dependent optical properties for semiconducting silicon carbide nanotubes," *Opt. Exp.*, vol. 15, no. 17, pp. 10947–10957, Aug. 2007.

[103] C. Pham-Huu, N. Keller, G. Ehret, and M. J. Ledoux, "The first preparation of silicon carbide nanotubes by shape memory synthesis and their catalytic potential," *J. Catalysis*, vol. 200, no. 2, pp. 400–410, Jun. 2001.

[104] J.-X. Zhao and Y.-H. Ding, "Silicon carbide nanotubes functionalized by transition metal atoms: A density-functional study," *J. Phys. Chem. C*, vol. 112, no. 7, pp. 2558–2564, Feb. 2008.

[105] X. Wang and K. M. Liew, "Density functional study of fluorinated single-walled silicon carbide nanotubes," *J. Phys. Chem. C*, vol. 116, no. 2, pp. 1702–1708, Jan. 2012.

[106] Y. Arntz *et al.*, "Label-free protein assay based on a nanomechanical cantilever array," *Nanotechnology*, vol. 14, no. 1, pp. 86–90, Jan. 2003.

[107] K. A. Stevenson, A. Mehta, P. Sachenko, K. M. Hansen, and T. Thundat, "Nanomechanical effect of enzymatic manipulation of DNA on microcantilever surfaces," *Langmuir*, vol. 18, no. 23, pp. 8732–8736, Nov. 2002.

[108] B. Ilic, D. Czaplewski, H. G. Craighead, P. Neuzil, C. Campagnolo, and C. Batt, "Mechanical resonant immunospecific biological detector," *Appl. Phys. Lett.*, vol. 77, no. 3, p. 450, Jul. 2000.

[109] B. Ilic, Y. Yang, and H. G. Craighead, "Virus detection using nanoelectromechanical devices," *Appl. Phys. Lett.*, vol. 85, no. 13, p. 2604, 2004.

[110] K. Y. Gfeller, N. Nugaeva, and M. Hegner, "Rapid biosensor for detection of antibiotic-selective growth of *Escherichia coli*," *Appl. Environ. Microbiol.*, vol. 71, no. 5, pp. 2626–2631, Apr. 2005.

[111] N. Nugaeva, K. Y. Gfeller, N. Backmann, H. P. Lang, M. Düggelin, and M. Hegner, "Micromechanical cantilever array sensors for selective fungal immobilization and fast growth detection," *Biosensors Bioelectron.*, vol. 21, no. 6, pp. 849–856, Dec. 2004.

[112] C. A. Savran, S. M. Knudsen, A. D. Ellington, and S. R. Manalis, "Micromechanical detection of proteins using aptamer-based receptor molecules," *Anal. Chem.*, vol. 76, no. 11, pp. 3194–3198, Jun. 2004.

[113] Y. Lin and S. D. Jayasena, "Inhibition of multiple thermostable DNA polymerases by a heterodimeric aptamer," *J. Molecular Biol.*, vol. 271, no. 1, pp. 100–111, Aug. 1997.

[114] A. Subramanian *et al.*, "Glucose biosensing using an enzyme-coated microcantilever," *Appl. Phys. Lett.*, vol. 81, no. 2, p. 385, Jul. 2002.

[115] J. Pei, F. Tian, and T. Thundat, "Glucose biosensor based on the microcantilever," *Anal. Chem.*, vol. 76, no. 2, pp. 292–297, Jan. 2004.

[116] X. Yan, H.-F. Ji, and Y. Lvov, "Modification of microcantilevers using layer-by-layer nanoassembly film for glucose measurement," *Chem. Phys. Lett.*, vol. 396, no. 1, pp. 34–37, Sep. 2004.

[117] U. Starke *et al.*, "The (0001)-surface of 6H-SiC: Morphology, composition and structure," *App. Surf. Sci.*, vol. 89, no. 2, pp. 175–185, Jun. 1995.

[118] S. Nishino, J. A. Powell, and H. A. Will, "Production of large-area single-crystal wafers of cubic SiC for semiconductor devices," *Appl. Phys. Lett.*, vol. 42, no. 5, p. 460, 1983.

[119] C. Coletti, *Silicon Carbide Biocompatibility, Surface Control, and Electronic Cellular Interaction for Biosensing Applications*. Ann Arbor, MI, USA: ProQuest, 2007.

[120] M. Levinshtein, S. Rumyantsev, and M. S. Shur, *Special Issue: SiC Materials and Devices*. Singapore: World Scientific, 2006.

[121] S. E. Saddow and A. Agarwal, *Advances in Silicon Carbide Processing and Applications*. Norwood, MA, USA: Artech House, 2004.

[122] M. E. Lin *et al.*, "GaN grown on hydrogen plasma cleaned 6H-SiC substrates," *Appl. Phys.*, vol. 62, no. 7, p. 702, 1993.

[123] M. Mehregany, C. A. Zorman, N. Rajan, and C. H. Wu, "Silicon carbide MEMS for harsh environments," *Proc. IEEE*, vol. 86, no. 8, pp. 1594–1609, Aug. 1998.

[124] Y. T. Yang *et al.*, "Monocrystalline silicon carbide nanoelectromechanical systems," *Appl. Phys. Lett.*, vol. 78, no. 2, p. 162, 2001.

[125] A. Oliveros, A. Guiseppi-Elie, and S. E. Saddow, "Silicon carbide: A versatile material for biosensor applications," *Biomed. Microdevices*, vol. 15, no. 2, pp. 353–368, Apr. 2013.

[126] C. Locke *et al.*, "3C-SiC films on Si for MEMS applications: Mechanical properties," *Mater. Sci. Forum*, vols. 615–617, pp. 633–636, Mar. 2009.

[127] A. Ellison *et al.*, "High temperature CVD growth of SiC," *Mater. Sci. Eng. B*, vols. 61–62, pp. 113–120, Jul. 1998.

[128] T. Seyller, "Passivation of hexagonal SiC surfaces by hydrogen termination," *J. Phys., Condens. Matter*, vol. 16, no. 17, pp. S1755–S1782, Apr. 2004.

[129] C. Locke, C. Frewin, L. Abbati, and S. E. Saddow, "Demonstration of 3C-SiC MEMS structures on polysilicon-on-oxide substrates," *MRS Proc.*, vol. 1246, p. 1246-B08-05, Feb. 2011.

[130] C. A. Zorman *et al.*, "Epitaxial growth of 3C–SiC films on 4 in. diam (100) silicon wafers by atmospheric pressure chemical vapor deposition," *J. Appl. Phys.*, vol. 78, no. 8, pp. 5136–5138, Oct. 1995.

[131] M. Syväjärvi *et al.*, "Liquid phase epitaxial growth of SiC," *J. Crystal Growth*, vol. 197, nos. 1–2, pp. 147–154, Feb. 1998.

[132] J. Chen, A. J. Steckl, and M. J. Loboda, "Molecular beam epitaxy growth of SiC on Si(111) from silacyclobutane," *J. Vac. Sci. Technol. B*, vol. 16, no. 3, pp. 1305–1308, May 1998.

[133] M. Reyes, Y. Shishkin, S. Harvey, and S. E. Saddow, "Increased growth rates of 3C-SiC on Si (100) substrates via HCl growth additive," *Mater. Sci. Forum*, vols. 556–557, pp. 191–194, Sep. 2007.

[134] R. Yakimova, R. M. Petoral, Jr., G. R. Yazdi, C. Vahlberg, A. L. Spetz, and K. Uvdal, "Surface functionalization and biomedical applications based on SiC," *J. Phys. D, Appl. Phys.*, vol. 40, no. 20, pp. 6435–6442, Oct. 2007.

[135] X. Li, X. Wang, R. Bondokov, J. Morris, Y. H. An, and T. S. Sudarshan, "Micro/nanoscale mechanical and tribological characterization of SiC for orthopedic applications," *J. Biomed. Mater. Res. B, Appl. Biomater.*, vol. 72B, no. 2, pp. 353–361, Feb. 2005.

[136] G. L. Harris, *Properties of Silicon Carbide. London: INSPEC, 1995*, pp. 1–297.

[137] C. H. Li, I. B. Bhat, R. Wang, and J. Seiler, "Electro-chemical mechanical polishing of silicon carbide," *J. Electron. Mater.*, vol. 33, no. 5, pp. 481–486, May 2004.

[138] L. Zhou, V. Audurier, P. Pirouz, and J. A. Powell, "Chemomechanical polishing of silicon carbide," *J. Electrochem. Soc.*, vol. 144, no. 6, pp. L161–L163, Jun. 1997.

[139] C.-M. Zetterling, *Process Technology for Silicon Carbide Devices*. Edison, NJ, USA: IET, 2002.

[140] J. Bernhardt, J. Schardt, U. Starke, and K. Heinz, "Epitaxially ideal oxide–semiconductor interfaces: Silicate adlayers on hexagonal (0001) and $(000\bar{1})(000\bar{1})$ SiC surfaces," *Appl. Phys. Lett.*, vol. 74, no. 8, pp. 1084–1086, 1999.

[141] S. Soubatch, S. E. Saddow, S. P. Rao, W. Y. Lee, M. Konuma, and U. Starke, "Structure and morphology of 4H-SiC wafer surfaces after H_2-etching," *Mater. Sci. Forum*, vols. 483–485, pp. 761–764, May 2005.

[142] X. L. Wu, J. Y. Fan, T. Qiu, X. Yang, G. G. Siu, and P. K. Chu, "Experimental evidence for the quantum confinement effect in 3*C*-SiC nanocrystallites," *Phys. Rev. Lett.*, vol. 94, no. 2, p. 026102, Jan. 2005.

[143] J. Botsoa, J. M. Bluet, V. Lysenko, O. Marty, D. Barbier, and G. Guillot, "Photoluminescence of 6H-SiC nanostructures fabricated by electrochemical etching," *J. Appl. Phys.*, vol. 102, no. 8, p. 083526, 2007.

[144] H. Lin, J. A. Gerbec, M. Sushchikh, and E. W. McFarland, "Synthesis of amorphous silicon carbide nanoparticles in a low temperature low pressure plasma reactor," *Nanotechnology*, vol. 19, no. 32, p. 325601, Jul. 2008.

[145] Y. Leconte, M. Leparoux, X. Portier, and N. Herlin-Boime, "Controlled synthesis of β-SiC nanopowders with variable stoichiometry using inductively coupled plasma," *Plasma Chem. Plasma Process.*, vol. 28, no. 2, pp. 233–248, Apr. 2008.

[146] S. Yang, H. Zeng, H. Zhao, H. Zhang, and W. Cai, "Luminescent hollow carbon shells and fullerene-like carbon spheres produced by laser ablation with toluene," *J. Mater. Chem.*, vol. 21, no. 12, pp. 4432–4436, 2011.

[147] J. Botsoa, V. Lysenko, A. Góloën, O. Marty, J. M. Bluet, and G. Guillot, "Application of 3*C*-Si*C* quantum dots for living cell imaging," *Appl. Phys. Lett.*, vol. 92, no. 17, p. 173902, 2008.

[148] E. H. Williams *et al.*, "Immobilization of streptavidin on 4H–SiC for biosensor development," *Appl. Surf. Sci.*, vol. 258, no. 16, pp. 6056–6063, Jun. 2012.

[149] S. Brahim, A. M. Wilson, D. Narinesingh, E. Iwuoha, and A. Guiseppi-Elie, "Chemical and biological sensors based on electrochemical detection using conducting electroactive polymers," *Microchim. Acta*, vol. 143, no. 2, pp. 123–137, Dec. 2003.
[150] R. M. Petoral, Jr., G. R. Yazdi, A. L. Spetz, R. Yakimova, and K. Uvdal, "Organosilane-functionalized wide band gap semiconductor surfaces," *Appl. Phys. Lett.*, vol. 90, no. 22, p. 223904, 2007.
[151] M. Stutzmann, J. A. Garrido, M. Eickhoff, and M. S. Brandt, "Direct biofunctionalization of semiconductors: A survey," *Phys. Status Solidi A*, vol. 203, no. 14, pp. 3424–3437, Nov. 2006.
[152] T. Matsuo, M. Esashi, and H. Abe, "ISFET's using inorganic gate thin films," *IEEE Trans. Electron Devices*, vol. 26, no. 12, pp. 1939–1944, Dec. 1979.
[153] C. Jakobson, I. Bloom, and Y. Nemirovsky, "*1/f* noise in CMOS transistors for analog applications from subthreshold to saturation," *Solid-State Electron.*, vol. 42, no. 10, pp. 1807–1817, Oct. 1998.
[154] A. L. Spetz *et al.*, "New transducer material concepts for biosensors and surface functionalization," *Proc. SPIE*, vol. 7362, p. 736206, May 2009.
[155] S. J. Schoell *et al.*, "Functionalization of 6*H*-SiC surfaces with organosilanes," *Appl. Phys. Lett.*, vol. 92, no. 15, p. 153301, 2008.
[156] S. Dhar, O. Seitz, M. D. Halls, S. Choi, Y. J. Chabal, and L. C. Feldman, "Chemical properties of oxidized silicon carbide surfaces upon etching in hydrofluoric acid," *J. Amer. Chem. Soc.*, vol. 131, no. 46, pp. 16808–16813, Nov. 2009.
[157] M. Preuss, F. Bechstedt, W. G. Schmidt, Jr., J. Sochos, B. Schröter, and W. Richter, "Clean and pyrrole-functionalized Si- and C-terminated SiC surfaces: First-principles calculations of geometry and energetics compared with LEED and XPS," *Phys. Rev. B*, vol. 74, no. 2, p. 235406, Dec. 2006.
[158] A. Catellani and G. Cicero, "Modifications of cubic SiC surfaces studied by *ab initio* simulations: From gas adsorption to organic functionalization," *J. Phys. D, Appl. Phys.*, vol. 40, no. 20, pp. 6215–6224, Oct. 2007.
[159] G. Cicero and A. Catellani, "Towards SiC surface functionalization: An *ab initio* study," *J. Chem. Phys.*, vol. 122, no. 21, p. 214716, 2005.
[160] P. Godignon, "SiC materials and technologies for sensors development," *Mater. Sci. Forum*, vols. 483–485, pp. 1009–1014, May 2005.
[161] P. Godignon, I. Martin, G. Gabriel, R. Gömez, M. Placidi, and R. Villa, "New generation of SiC based biodevices implemented on 4' wafers," *Mater. Sci. Forum*, vols. 645–648, pp. 1097–1100, Apr. 2010.
[162] H. O. Pierson, *Handbook of Chemical Vapor Deposition*, 2nd ed. Norwich, NY, USA: William Andrew, 1999.
[163] G. Gabriel *et al.*, "Manufacturing and full characterization of silicon carbide-based multi-sensor micro-probes for biomedical applications," *Microelectron. J.*, vol. 38, no. 3, pp. 406–415, Mar. 2007.
[164] H. Tsuchida, I. Kamata, and K. Izumi, "Infrared attenuated total reflection spectroscopy of 6H-SiC(0001) and (000(1)over-bar) surfaces," *J. Appl. Phys.*, vol. 85, no. 7, pp. 3569–3575, 1999.
[165] N. G. Wright and A. B. Horsfall, "SiC sensors: A review," *J. Phys. D, Appl. Phys.*, vol. 40, no. 20, pp. 6345–6354, 2007.
[166] N. Marsi, B. Y. Majlis, A. A. Hamzah, and F. Mohd-Yasin, "The mechanical and electrical effects of MEMS capacitive pressure sensor based 3C-SiC for extreme temperature," *J. Eng.*, vol. 2014, May 2014, Art. ID 715167.
[167] M. J. Madou, *Fundamentals of Microfabrication*. Boca Raton, FL, USA: CRC Press, 2002.
[168] J. Mertens, M. Álvarez, and J. Tamayo, "Real-time profile of microcantilevers for sensing applications," *Appl. Phys. Lett.*, vol. 87, no. 23, p. 234102, 2005.
[169] S. Chatzandroulis, A. Tserepi, D. Goustouridis, P. Normand, and D. Tsoukalas, "Fabrication of single crystal Si cantilevers using a dry release process and application in a capacitive-type humidity sensor," *Microelectron. Eng.*, vols. 61–62, pp. 955–961, Jul. 2002.
[170] A. R. Kermany, G. Brawley, N. Mishra, E. Sheridan, W. P. Bowen, and F. Iacopi, "Microresonators with *Q*-factors over a million from highly stressed epitaxial silicon carbide on silicon," *Appl. Phys. Lett.*, vol. 104, no. 8, p. 081901, Feb. 2014.
[171] F. Iacopi, R. E. Brock, A. Iacopi, L. Hold, and R. H. Dauskardt, "Evidence of a highly compressed nanolayer at the epitaxial silicon carbide interface with silicon," *Acta Mater.*, vol. 61, no. 17, pp. 6533–6540, Oct. 2013.
[172] L. Sekaric, J. M. Parpia, H. G. Craighead, T. Feygelson, B. H. Houston, and J. E. Butler, "Nanomechanical resonant structures in nanocrystalline diamond," *Appl. Phys. Lett.*, vol. 81, no. 23, p. 4455, 2002.
[173] M. Placidi *et al.*, "Fabrication of monocrystalline 3C–SiC resonators for MHz frequency sensors applications," *Sens. Actuators B, Chem.*, vol. 133, no. 1, pp. 276–280, Jul. 2008.
[174] S. Schmid, Jr., K. D. Jensen, K. H. Nielsen, and A. Boisen, "Damping mechanisms in high-*Q* micro and nanomechanical string resonators," *Phys. Rev. B*, vol. 84, no. 1, p. 165307, Oct. 2011.
[175] M. Houmad, A. Abbassi, A. Benyoussef, H. Ez-Zahraouy, and A. El Kenz, "Optical properties of Ni doped 3C-SiC with *ab initio* calculations," presented at the Int. Renew. Sustain. Energy Conf. (IRSEC), Oct. 2014, pp. 596–601.
[176] X. Wang and K. M. Liew, "Silicon carbide nanotubes serving as a highly sensitive gas chemical sensor for formaldehyde," *J. Phys. Chem. C*, vol. 115, no. 21, pp. 10388–10393, Jun. 2011.
[177] M. Wijesundara and R. Azevedo, *Silicon Carbide Microsystems for Harsh Environments*. Springer-Verlag New York, 2011.
[178] B. V. Cunning, M. Ahmed, N. Mishra, A. R. Kermany, B. Wood, and F. Iacopi, "Graphitized silicon carbide microbeams: Wafer-level, self-aligned graphene on silicon wafers," *Nanotechnology*, vol. 25, no. 32, p. 325301, Jul. 2014.
[179] B. Gupta, M. Notarianni, N. Mishra, M. Shafiei, F. Iacopi, and N. Motta, "Evolution of epitaxial graphene layers on 3C SiC/Si (111) as a function of annealing temperature in UHV," *Carbon*, vol. 68, pp. 563–572, Mar. 2014.
[180] B. Gupta, E. Placidi, C. Hogan, N. Mishra, F. Iacopi, and N. Motta, "The transition from 3C SiC (111) to graphene captured by ultra high vacuum scanning tunneling microscopy," *Carbon*, vol. 91, pp. 378–385, Sep. 2015.
[181] V. Singh, D. Joung, L. Zhai, S. Das, S. I. Khondaker, and S. Seal, "Graphene based materials: Past, present and future," *Prog. Mater. Sci.*, vol. 56, no. 8, pp. 1178–1271, Oct. 2011.
[182] K. S. Novoselov *et al.*, "Electric field effect in atomically thin carbon films," *Science*, vol. 306, no. 5696, pp. 666–669, Oct. 2004.
[183] K. S. Novoselov *et al.*, "Room-temperature quantum Hall effect in graphene," *Science*, vol. 315, no. 5817, p. 1379, Mar. 2007.
[184] Y. Zhang, Y.-W. Tan, H. L. Stormer, and P. Kim, "Experimental observation of the quantum Hall effect and Berry's phase in graphene," *Nature*, vol. 438, no. 7, pp. 201–204, Nov. 2005.
[185] S. V. Morozov *et al.*, "Strong suppression of weak localization in graphene," *Phys. Rev. Lett.*, vol. 97, no. 1, p. 016801, Jul. 2006.
[186] W. Choi, I. Lahiri, R. Seelaboyina, and Y. S. Kang, "Synthesis of graphene and its applications: A review," *Critical Rev. Solid State Mater. Sci.*, vol. 35, no. 1, pp. 52–71, Feb. 2010.
[187] A. A. Balandin *et al.*, "Superior thermal conductivity of single-layer graphene," *Nano Lett.*, vol. 8, no. 3, pp. 902–907, 2008.
[188] J.-H. Chen, C. Jang, S. Xiao, M. Ishigami, and M. S. Fuhrer, "Intrinsic and extrinsic performance limits of graphene devices on SiO_2," *Nature Nanotechnol.*, vol. 3, no. 4, pp. 206–209, Mar. 2008.
[189] N. O. Weiss *et al.*, "Graphene: An emerging electronic material," *Adv. Mater.*, vol. 24, no. 43, pp. 5782–5825, Nov. 2012.
[190] K. S. Novoselov *et al.*, "Two-dimensional gas of massless Dirac fermions in graphene," *Nature*, vol. 438, no. 7065, pp. 197–200, Nov. 2005.
[191] Q. Bao and K. P. Loh, "Graphene photonics, plasmonics, and broadband optoelectronic devices," *ACS Nano*, vol. 6, no. 5, pp. 3677–3694, May 2012.
[192] W. C. Lee *et al.*, "Origin of enhanced stem cell growth and differentiation on graphene and graphene oxide," *ACS Nano*, vol. 5, no. 9, pp. 7334–7341, Sep. 2011.
[193] P. Orlita *et al.*, "Approaching the Dirac point in high-mobility multilayer epitaxial graphene," *Phys. Rev. Lett.*, vol. 101, p. 267601, Dec. 2008.
[194] C. Lee, X. Wei, J. W. Kysar, and J. Hone, "Measurement of the elastic properties and intrinsic strength of monolayer graphene," *Science*, vol. 321, no. 5887, pp. 385–388, Jul. 2008.
[195] X. Li, X. Wang, L. Zhang, S. Lee, and H. Dai, "Chemically derived, ultrasmooth graphene nanoribbon semiconductors," *Science*, vol. 319, no. 5867, pp. 1229–1232, Feb. 2008.
[196] K. A. Ritter and J. W. Lyding, "The influence of edge structure on the electronic properties of graphene quantum dots and nanoribbons," *Nature Mater.*, vol. 8, no. 3, pp. 235–242, Feb. 2009.
[197] A. M. Pinto, I. C. Gonçalves, and F. D. Magalhães, "Graphene-based materials biocompatibility: A review," *Colloids Surf. B, Biointerfaces*, vol. 111, pp. 188–202, Nov. 2013.
[198] V. Dhand, K. Y. Rhee, H. J. Kim, and D. H. Jung, "A comprehensive review of graphene nanocomposites: Research status and trends," *J. Nanomater.*, vol. 2013, Jan. 2013, Art. ID 158.

[199] K.-H. Liao, Y.-S. Lin, C. W. Macosko, and C. L. Haynes, "Cytotoxicity of graphene oxide and graphene in human erythrocytes and skin fibroblasts," *ACS Appl. Mater. Interfaces*, vol. 3, no. 7, pp. 2607–2615, Jun. 2011.

[200] S. Liu *et al.*, "Antibacterial activity of graphite, graphite oxide, graphene oxide, and reduced graphene oxide: Membrane and oxidative stress," *ACS Nano*, vol. 5, no. 9, pp. 6971–6980, Sep. 2011.

[201] R. M. Donlan, "Biofilms and device-associated infections," *Emerg. Infectious Diseases*, vol. 7, no. 2, pp. 277–281, Mar. 2001.

[202] H. Anwar, J. L. Strap, K. Chen, and J. W. Costerton, "Dynamic interactions of biofilms of mucoid Pseudomonas aeruginosa with tobramycin and piperacillin," *Antimicrob. Agents. Chemother.*, vol. 36, no. 6, pp. 1208–1214, May 1992.

[203] M. Gabriel, K. Nazmi, E. C. Veerman, A. V. N. Amerongen, and A. Zentner, "Preparation of LL-37-grafted titanium surfaces with bactericidal activity," *Bioconjugate Chem.*, vol. 17, no. 2, pp. 548–550, Jan. 2006.

[204] C. M. Santos, M. C. R. Tria, R. A. M. V. Vergara, F. Ahmed, R. C. Advincula, and D. F. Rodrigues, "Antimicrobial graphene polymer (PVK-GO) nanocomposite films," *Chem. Commun.*, vol. 47, no. 31, pp. 8892–8894, Aug. 2011.

[205] I. E. M. Carpio, C. M. Santos, X. Wei, and D. F. Rodrigues, "Toxicity of a polymer–graphene oxide composite against bacterial planktonic cells, biofilms, and mammalian cells," *Nanoscale*, vol. 4, no. 15, pp. 4746–4756, Aug. 2012.

[206] E. Peng *et al.*, "Synthesis of manganese ferrite/graphene oxide nanocomposites for biomedical applications," *Small*, vol. 8, no. 23, pp. 3620–3630, Dec. 2012.

[207] W. C. Lee, C. H. Lim, C. S. Kenry, K. P. Loh, and C. T. Lim, "Cell-assembled graphene biocomposite for enhanced chondrogenic differentiation," *Small*, vol. 11, no. 8, pp. 963–969, Jan. 2015.

[208] A. Reina *et al.*, "Large area, few-layer graphene films on arbitrary substrates by chemical vapor deposition," *Nano Lett.*, vol. 9, no. 1, pp. 30–35, Dec. 2008.

[209] A. K. Geim and K. S. Novoselov, "The rise of graphene," *Nature Mater.*, vol. 6, no. 3, pp. 183–191, Mar. 2007.

[210] P. R. Somani, S. P. Somani, and M. Umeno, "Planer nano-graphenes from camphor by CVD," *Chem. Phys. Lett.*, vol. 430, nos. 1–3, pp. 56–59, 2006.

[211] J. Wang, M. Zhu, R. A. Outlaw, X. Zhao, D. M. Manos, and B. C. Holloway, "Synthesis of carbon nanosheets by inductively coupled radio-frequency plasma enhanced chemical vapor deposition," *Carbon*, vol. 42, no. 14, pp. 2867–2872, 2004.

[212] A. N. Obraztsov, A. A. Zolotukhin, A. O. Ustinov, A. P. Volkov, Y. Svirko, and K. Jefimovs, "DC discharge plasma studies for nanostructured carbon CVD," *Diamond Rel. Mater.*, vol. 12, nos. 3–7, pp. 917–920, 2003.

[213] S. Stankovich *et al.*, "Synthesis of graphene-based nanosheets via chemical reduction of exfoliated graphite oxide," *Carbon*, vol. 45, no. 7, pp. 1558–1565, 2007.

[214] S. Gilje, S. Han, M. Wang, K. L. Wang, and R. B. Kaner, "A chemical route to graphene for device applications," *Nano Lett.*, vol. 7, no. 11, pp. 3394–3398, Nov. 2007.

[215] D. V. Kosynkin *et al.*, "Longitudinal unzipping of carbon nanotubes to form graphene nanoribbons," *Nature*, vol. 458, no. 7240, pp. 872–876, Apr. 2009.

[216] H. Santos, L. Chico, and L. Brey, "Carbon nanoelectronics: Unzipping tubes into graphene ribbons," *Phys. Rev. Lett.*, vol. 103, p. 086801, Aug. 2009.

[217] L. Jiao, L. Zhang, X. Wang, G. Diankov, and H. Dai, "Narrow graphene nanoribbons from carbon nanotubes," *Nature*, vol. 458, no. 7240, pp. 877–880, Apr. 2009.

[218] A. Sinitskii, A. Dimiev, D. V. Kosynkin, and J. M. Tour, "Graphene nanoribbon devices produced by oxidative unzipping of carbon nanotubes," *ACS Nano*, vol. 4, no. 9, pp. 5405–5413, Sep. 2010.

[219] H. Kageshima, H. Hibino, and S. Tanabe, "The physics of epitaxial graphene on SiC(0001)," *J. Phys., Condens. Matter*, vol. 24, no. 31, p. 314215, 2012.

[220] A. Ouerghi *et al.*, "Large-area and high-quality epitaxial graphene on off-axis SiC wafers," *ACS Nano*, vol. 6, no. 7, pp. 6075–6082, Jun. 2012.

[221] G. Eda, G. Fanchini, and M. Chhowalla, "Large-area ultrathin films of reduced graphene oxide as a transparent and flexible electronic material," *Nature Nanotechnol.*, vol. 3, no. 5, pp. 270–274, Apr. 2008.

[222] H. A. Becerril, J. Mao, Z. Liu, R. M. Stoltenberg, Z. Bao, and Y. Chen, "Evaluation of solution-processed reduced graphene oxide films as transparent conductors," *ACS Nano*, vol. 2, no. 3, pp. 463–470, Mar. 2008.

[223] Y.-W. Son, M. L. Cohen, and S. G. Louie, "Energy gaps in graphene nanoribbons," *Phys. Rev. Lett.*, vol. 97, no. 21, p. 216803, Nov. 2006.

[224] V. Barone, O. Hod, and G. E. Scuseria, "Electronic structure and stability of semiconducting graphene nanoribbons," *Nano Lett.*, vol. 6, no. 12, pp. 2748–2754, Dec. 2006.

[225] T. Shimizu *et al.*, "Large intrinsic energy bandgaps in annealed nanotube-derived graphene nanoribbons," *Nature Nanotechnol.*, vol. 6, no. 1, pp. 45–50, Dec. 2010.

[226] M. Y. Han, B. Özyilmaz, Y. Zhang, and P. Kim, "Energy band-gap engineering of graphene nanoribbons," *Phys. Rev. Lett.*, vol. 98, no. 20, p. 206805, May 2007.

[227] A. L. Elías *et al.*, "Longitudinal cutting of pure and doped carbon nanotubes to form graphitic nanoribbons using metal clusters as nanoscalpels," *Nano Lett.*, vol. 10, no. 2, pp. 366–372, Feb. 2010.

[228] J. L. Tedesco *et al.*, "Hall effect mobility of epitaxial graphene grown on silicon carbide," *Appl. Phys. Lett.*, vol. 95, no. 12, p. 122102, 2009.

[229] P. Xu, H. Yu, X. Xia, F. Yu, M. Liu, and X. Li, "Resonant cantilevers with nanoparticles-spaced functional graphene-oxide sheets for high-performance sensing to ppt-level explosive vapor," in *Proc. IEEE 26th Int. Conf. Micro Electro Mech. Syst.*, Jan. 2013, pp. 989–992.

[230] J. Kang *et al.*, "Efficient transfer of large-area graphene films onto rigid substrates by hot pressing," *ACS Nano*, vol. 6, no. 6, pp. 5360–5365, Jun. 2012.

[231] J. D. Caldwell *et al.*, "Technique for the dry transfer of epitaxial graphene onto arbitrary substrates," *ACS Nano*, vol. 4, no. 2, pp. 1108–1114, Oct. 2009. [Online]. Available: http://arxiv.org/abs/0910.2624

[232] F. Iacopi *et al.*, "A catalytic alloy approach for graphene on epitaxial SiC on silicon wafers," *J. Mater. Res.*, vol. 30, no. 5, pp. 609–616, Feb. 2015.

[233] P. Macháč, T. Fidler, S. Cichoň, and V. Jurka, "Synthesis of graphene on Co/SiC structure," *J. Mater. Sci., Mater. Electron.*, vol. 24, no. 10, pp. 3793–3799, 2013.

[234] T. Yoneda, M. Shibuya, K. Mitsuhara, A. Visikovskiy, Y. Hoshino, and Y. Kido, "Graphene on SiC(0001) and SiC(000$\bar{1}$) surfaces grown via Ni-silicidation reactions," *Surf. Sci.*, vol. 604, nos. 17–18, pp. 1509–1515, Aug. 2010.

[235] A. J. Van Bommel, J. E. Crombeen, and A. Van Tooren, "LEED and Auger electron observations of the SiC(0001) surface," *Surf. Sci.*, vol. 48, no. 2, pp. 463–472, Mar. 1975.

[236] E. Rollings *et al.*, "Synthesis and characterization of atomically thin graphite films on a silicon carbide substrate," *J. Phys. Chem. Solids*, vol. 67, nos. 9–10, pp. 2172–2177, Sep./Oct. 2006.

[237] Z.-Y. Juang *et al.*, "Synthesis of graphene on silicon carbide substrates at low temperature," *Carbon*, vol. 47, no. 8, pp. 2026–2031, 2009.

[238] E. Escobedo-Cousin *et al.*, "Local solid phase growth of few-layer graphene on silicon carbide from nickel silicide supersaturated with carbon," *J. Appl. Phys.*, vol. 113, no. 11, p. 114309, Mar. 2013.

[239] C. Berger *et al.*, "Ultrathin epitaxial graphite: 2D electron gas properties and a route toward graphene-based nanoelectronics," *J. Phys. Chem. B*, vol. 108, no. 52, pp. 19912–19916, Dec. 2004.

[240] C. Berger *et al.*, "Electronic confinement and coherence in patterned epitaxial graphene," *Science*, vol. 312, no. 5777, pp. 1191–1196, May 2006.

[241] J. Penuelas *et al.*, "Surface morphology and characterization of thin graphene films on SiC vicinal substrate," *Phys. Rev. B*, vol. 79, no. 3, p. 033408, Jan. 2009.

[242] K. V. Emtsev *et al.*, "Towards wafer-size graphene layers by atmospheric pressure graphitization of silicon carbide," *Nature Mater.*, vol. 8, no. 3, pp. 203–207, Feb. 2009.

[243] T. Ohta, N. C. Bartelt, S. Nie, K. Thürmer, and G. L. Kellogg, "Role of carbon surface diffusion on the growth of epitaxial graphene on SiC," *Phys. Rev. B*, vol. 81, no. 12, p. 121411(R), Mar. 2010.

[244] A. Lauwers *et al.*, "Materials aspects, electrical performance, and scalability of Ni silicide towards sub-0.13 μm technologies," *J. Vac. Sci. Technol. B*, vol. 19, no. 6, p. 2026, 2001.

[245] P. Macháč, T. Fidler, S. Cichoň, and L. Mišková, "Synthesis of graphene on SiC substrate via Ni-silicidation reactions," *Thin Solid Films*, vol. 520, no. 16, pp. 5215–5218, 2012.

[246] F. Iacopi *et al.*, "Orientation-dependent stress relaxation in hetero-epitaxial 3C-SiC films," *Appl. Phys. Lett.*, vol. 102, no. 1, p. 011908, 2013.
[247] V. Y. Aristov *et al.*, "Graphene synthesis on cubic SiC/Si wafers. perspectives for mass production of graphene-based electronic devices," *Nano Lett.*, vol. 10, no. 3, pp. 992–995, Mar. 2010.
[248] U. Starke, C. Coletti, K. Emtsev, A. A. Zakharov, T. Ouisse, and D. Chaussende, "Large area quasi-free standing monolayer graphene on 3C-SiC(111)," *Mater. Sci.*, vols. 717–720, pp. 617–620, May 2012.
[249] P. Sutter, "Epitaxial graphene: How silicon leaves the scene," *Nature Mater.*, vol. 8, no. 3, pp. 171–172, Feb. 2009.
[250] R. Takahashi *et al.*, "Low-energy-electron-diffraction and X-ray-photoelectron-spectroscopy studies of graphitization of 3C-SiC(111) thin film on Si(111) substrate," *Jpn. J. Appl. Phys.*, vol. 50, no. 7R, p. 070103, 2011.
[251] A. Bostwick *et al.*, "Symmetry breaking in few layer graphene films," *New J. Phys.*, vol. 9, no. 1, p. 385, Oct. 2007.
[252] A. Ouerghi *et al.*, "Structural coherency of epitaxial graphene on 3C-SiC(111) epilayers on Si(111)," *Appl. Phys. Lett.*, vol. 97, no. 16, p. 161905, Oct. 2010.
[253] A. Ouerghi *et al.*, "Sharp interface in epitaxial graphene layers on 3C-SiC(100)/Si(100) wafers," *Phys. Rev. B*, vol. 83, no. 20, p. 205429, 2011.
[254] K. V. Emtsev, F. Speck, T. Seyller, L. Ley, and J. D. Riley, "Interaction, growth, and ordering of epitaxial graphene on SiC{0001} surfaces: A comparative photoelectron spectroscopy study," *Phys. Rev. B*, vol. 77, no. 15, p. 155303, Apr. 2008.
[255] Z. H. Ni *et al.*, "Raman spectroscopy of epitaxial graphene on a SiC substrate," *Phys. Rev. B*, vol. 77, p. 115416, Mar. 2008.
[256] G. Kästle, H. G. Boyen, A. Schröder, A. Plettl, and P. Ziemann, "Size effect of the resistivity of thin epitaxial gold films," *Phys. Rev. B*, vol. 70, no. 1, p. 165414, Oct. 2004.
[257] T. Kuila, S. Bose, A. K. Mishra, P. Khanra, N. H. Kim, and J. H. Lee, "Chemical functionalization of graphene and its applications," *Prog. Mater. Sci.*, vol. 57, no. 7, pp. 1061–1105, Sep. 2012.
[258] M. Fang, K. Wang, H. Lu, Y. Yang, and S. Nutt, "Single-layer graphene nanosheets with controlled grafting of polymer chains," *J. Mater. Chem.*, vol. 20, no. 10, pp. 1982–1992, 2010.
[259] M. J. Park, J. K. Lee, B. S. Lee, Y.-W. Lee, I. S. Choi, and S.-G. Lee, "Covalent modification of multiwalled carbon nanotubes with imidazolium-based ionic liquids: Effect of anions on solubility," *Chem. Mater.*, vol. 18, no. 6, pp. 1546–1551, 2006.
[260] H. Yang *et al.*, "Covalent functionalization of chemically converted graphene sheets via silane and its reinforcement," *J. Mater. Chem.*, vol. 19, no. 26, pp. 4632–4638, 2009.
[261] A. B. Bourlinos, D. Gournis, D. Petridis, T. Szabó, A. Szeri, and I. Dékány, "Graphite oxide: Chemical reduction to graphite and surface modification with primary aliphatic amines and amino acids," *Langmuir*, vol. 19, no. 15, pp. 6050–6055, 2003.
[262] E. Bekyarova *et al.*, "Chemical modification of epitaxial graphene: Spontaneous grafting of aryl groups," *J. Amer. Chem. Soc.*, vol. 131, no. 4, pp. 1336–1337, Feb. 2009.
[263] Y. Zhu, A. L. Higginbotham, and J. M. Tour, "Covalent functionalization of surfactant-wrapped graphene nanoribbons," *Chem. Mater.*, vol. 21, no. 21, pp. 5284–5291, 2009.
[264] S. Stankovich, R. D. Piner, S. T. Nguyen, and R. S. Ruoff, "Synthesis and exfoliation of isocyanate-treated graphene oxide nanoplatelets," *Carbon*, vol. 44, no. 15, pp. 3342–3347, Dec. 2006.
[265] Z. Liu, J. T. Robinson, X. Sun, and H. Dai, "PEGylated nanographene oxide for delivery of water-insoluble cancer drugs," *J. Amer. Chem. Soc.*, vol. 130, no. 33, pp. 10876–10877, Aug. 2008.
[266] S. Vadukumpully, J. Gupta, Y. Zhang, G. Q. Xu, and S. Valiyaveettil, "Functionalization of surfactant wrapped graphene nanosheets with alkylazides for enhanced dispersibility," *Nanoscale*, vol. 3, no. 1, pp. 303–308, Jan. 2011.
[267] X. Xu *et al.*, "Functionalization of graphene sheets by polyacetylene: Convenient synthesis and enhanced emission," *Macromolecular Chem. Phys.*, vol. 212, no. 8, pp. 768–773, 2011.
[268] T. Kuila *et al.*, "Preparation of functionalized graphene/linear low density polyethylene composites by a solution mixing method," *Carbon*, vol. 49, no. 3, pp. 1033–1037, Mar. 2011.
[269] C. Shan, H. Yang, D. Han, Q. Zhang, A. Ivaska, and L. Niu, "Water-soluble graphene covalently functionalized by biocompatible poly-L-lysine," *Langmuir*, vol. 25, no. 20, pp. 12030–12033, Oct. 2009.
[270] D.-D. Zhang, S.-Z. Zu, and B.-H. Han, "Inorganic–organic hybrid porous materials based on graphite oxide sheets," *Carbon*, vol. 47, no. 13, pp. 2993–3000, Nov. 2009.
[271] K. Yang, L. Feng, H. Hong, W. Cai, and Z. Liu, "Preparation and functionalization of graphene nanocomposites for biomedical applications," *Nature Protocols*, vol. 8, no. 12, pp. 2392–2403, Nov. 2013.

OREN COOPER received the bachelor's degree in biomedical science from Griffith University, in 2013. He is also completed the Honours thesis that was focused on developing novel array technologies, area where he has now over five years of experience. He was a recipient of the University Medallion for achieving the highest grade within his graduating year, and has since began his Ph.D. research project with the Institute for Glycomics, Griffith University, where he aims to develop novel label-free array technologies to explore complex biological interactions.

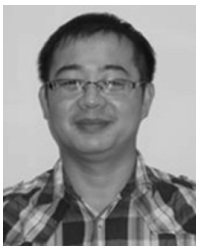

BEI WANG received the Ph.D. degree from the University of Technology, Sydney, in 2013, under the supervision of Prof. G. Wang to explore graphene-based materials for various energy storage devices, such as lithium-ion batteries, supercapacitors, and lithium–sulfur batteries. Since 2012, he has been involved in an ARC Linkage Project with the Australian Institute for Bioengineering and Nanotechnology, University of Queensland, as a Post-Doctoral Research Fellow to develop high-performance cathode materials for lithium-ion batteries. In 2014, he joined the Associate Professor Francesca Iacopi's Group as a Griffith University Post-Doctoral Research Fellow and his work now is focused on the growth of self-aligned graphene for biosensing and on-chip energy storage applications.

CHRISTOPHER L. BROWN received the bachelor's degree in chemistry and the Ph.D. degree in molecular recognition, self-assembling systems, and molecular devices from the University of Sheffield, U.K., in 1991. He then travelled to Australia, where he spent three years, initially as a Royal Society Research Fellow and then an HB & FM Gritton Research Fellow with the School of Chemistry, University of Sydney, working on molecular recognition processes. Returning to the U.K. for two years, he was an EPSRC funded Researcher with the University of Birmingham in the area of molecular devices under the guidance of Prof. F. Stoddart. He was appointed as a Lecturer in Organic Chemistry with Griffith University, Australia, in 1997, and achieved the rank of Associate Professor in 2010. His current research interests include molecular devices, supramolecular chemistry, and carbon materials.

JOE TIRALONGO received the Ph.D. degree in biochemistry from Monash University, Australia, in 2001. He is currently an Internationally Recognized Glycobiologist, and more recently, he has become an Expert in the use of glycomics (glycan and lectin) arrays to explore mammalian and microbial glycoscience. In 2008, he established the Glycomics Array Facility and associated technologies with Griffith University, which represents the only facility of its type in the Southern Hemisphere. This unique expertise has led to the establishment of important national and international collaborations that has contributed to a significant body of work, including over 50 peer-reviewed publications, eight book chapters, and one book. He has also been awarded a number of prestigious fellowships, including from the Australian Research Council (ARC), and his research has attracted national (ARC, Cancer Council, Ian Potter Foundation) and international (Association for International Cancer Research, Deutsche Forschungsgemeinschaft) competitive funding.

FRANCESCA IACOPI received the M.Sc. degree in physics from La Sapienza University, Rome, Italy, in 1996, and the Ph.D. degree in electrical engineering from the Katholieke Universiteit Leuven, Belgium, in 2004. She is currently a Materials Scientist and Nanotechnology Expert with over 15 years of research experience across the industry and academia. She has authored over 100 peer-reviewed publications and holds seven granted patents. She has achieved international reputation for her contributions to materials and processes for advanced CMOS technologies across the area of devices, interconnects, and packaging.

She was a Research Scientist with imec, Belgium, from 1999 to 2009. She held a year Guest Professorship with the University of Tokyo, Japan. From 2010 to 2011, she directed the Chip-Package Interaction strategy for GLOBALFOUNDRIES (CA, USA), the world's second -largest semiconductor foundry. At Griffith University, she was the inventor of a unique process for high-quality graphene on silicon, with applications in integrated microtechnologies, such as biocompatible sensing and energy storage.

She was a recipient of the 2003 Gold Graduate Student Award from MRS, a 2012 Future Fellowship from the Australian Research Council, and the Global Innovation Award for processes enabling low-cost graphene/silicon carbide MEMS in Washington, DC, in 2014.